Accepted Manuscript

Surmounting the resistance against EGFR inhibitors through the development of thieno[2,3-d]pyrimidine-based dual EGFR/HER2 inhibitors

Sandra N. Milik, Amal Kamal Abdel-Aziz, Deena S. Lasheen, Rabah A.T. Serya, Saverio Minucci, Khaled A.M. Abouzid

Solvent accessible region

Optimum enzymatic & Cellular activity

Optimum dual inhibition & cellular activity

Back Pocket

Hinge

EGFR: Met 793
HER2: Met 801

EGFR: Thr 854
HER2: Thr 862

EGFR IC$_{50}$ = 91.7 nM
HER2 IC$_{50}$ = 1.2 μM
A431 IC$_{50}$ = 1.45 μM
SKBr3 IC$_{50}$ = 4.83 μM
MDA-MB-361 IC$_{50}$ = 3.5 μM
NCI-H1975 IC$_{50}$ = 4.2 μM

Surmounting the resistance against EGFR inhibitors through the development of thieno[2,3-*d*]pyrimidine-based dual EGFR/HER2 inhibitors

Sandra N. Milik[1** †], Amal Kamal Abdel-Aziz[2,3 †], Deena S. Lasheen[1], Rabah A. T. Serya[1], Saverio Minucci[3,4], Khaled A. M. Abouzid[1*]

[1] Department of Pharmaceutical Chemistry, Faculty of Pharmacy, Ain Shams University, Abbassia, Cairo 11566, Egypt

[2] Department of Pharmacology and Toxicology, Faculty of Pharmacy, Ain Shams University, Abbassia, Cairo 11566, Egypt

[3] Department of Experimental Oncology, European Institute of Oncology, Via Adamello 16, 20139, Milan, Italy

[4] Department of Biosciences, University of Milan, Milan 20100, Italy

[†] These authors contributed equally to this work

* Correspondence: khaled.abouzid@pharma.asu.edu.eg

** Correspondence: Sandra.milik3@pharma.asu.edu.eg

ABSTRACT [1]

In light of the emergence of resistance against the currently available EGFR inhibitors, our study focuses on tackling this problem through the development of dual EGFR/HER2 inhibitors with improved enzymatic affinities. Guided by the binding mode of the marketed dual EGFR/HER2 inhibitor, Lapatinib, we proposed the design of dual EGFR/HER2 inhibitors based on the 6-phenylthieno[2,3-*d*]pyrimidine as a core scaffold and hinge binder. After two cycles of screening aiming to identify the optimum aniline headgroup and solubilizing group, we eventually identified **27b** as a dual EGFR/HER2 inhibitor with IC_{50} values of 91.7 nM and 1.2 μM, respectively. Notably, **27b** dramatically reduced the viability of various patient-derived cancer cells preferentially overexpressing EGFR/HER2 (A431, MDA-MBA-361 and SKBr3 with IC_{50} values of 1.45, 3.5 and 4.83 μM, respectively). Additionally, **27b** efficiently thwarted the proliferation of lapatinib-resistant human non-small lung carcinoma (NCI-H1975) cells, harboring T790M mutation, with IC_{50} of 4.2 μM. Consistently, **27b** significantly blocked EGF-induced EGFR activation and inactivated its downstream AKT/mTOR/S6 signaling pathway triggering apoptotic cell death in NCI-H1975 cells. The present study presents a promising candidate for further design and development of novel EGFR/HER2 inhibitors capable of overcoming EGFR TKIs resistance.

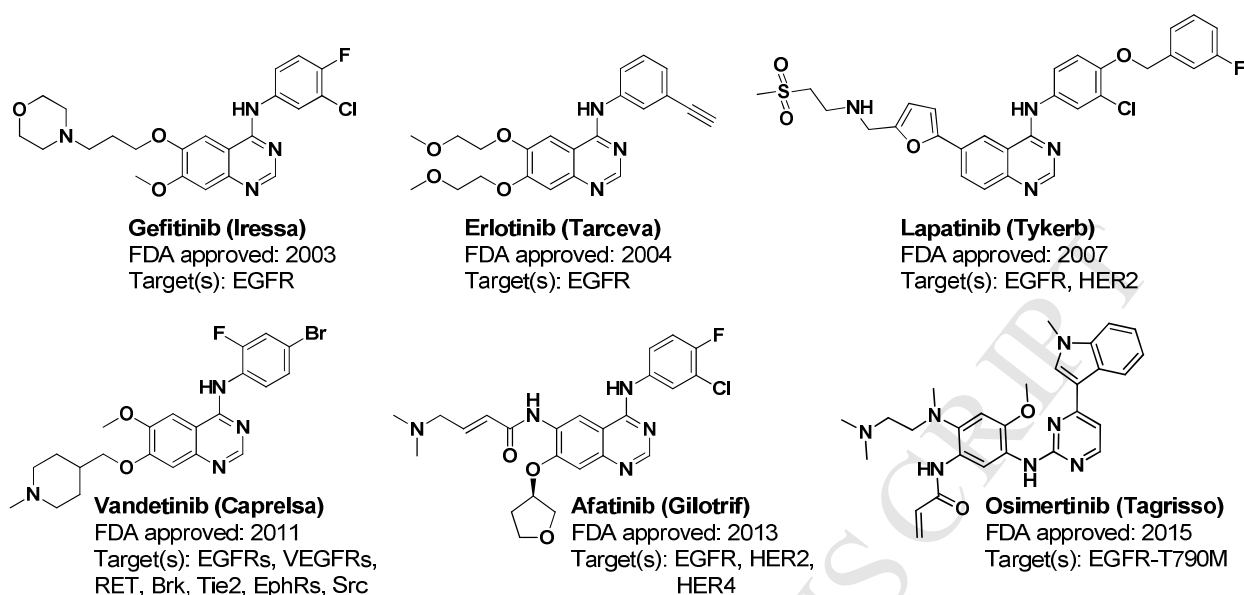**Keywords:** Dual EGFR/HER2 inhibitors, EGFR inhibitors Resistance, Thieno[2,3-*d*]pyrimidine

1. Introduction

The Epidermal Growth Factor Receptor (EGFR) family belongs to receptor tyrosine kinases (RTKs) which acts as a key regulator of diverse critical cellular functions pertaining to cell proliferation and differentiation [1]. The EGFR family comprises four structurally-related RTKs: EGFR (HER1), HER2, HER3 and HER4 [2–4]. Notably, EGFR dysregulation through either receptors overexpression or activating gain-of-function mutations [5,6], typically prompts proliferation upsurge, alters cell differentiation, confers apoptosis resistance and assists neoangiogenesis and metastasis, ultimately leading to tumorigenesis and progression (**Supplementary Figure S1**) [7,8]. Not surprisingly, EGFR dysregulation was reportedly associated with a number of the most lethal cancers worldwide such as non-small cell lung cancer (NSCLC), colorectal cancer, breast cancer and pancreatic cancer [5,8,9]. Consequently, promoted by the tremendous efforts invested in developing small molecule EGFR tyrosine kinase inhibitors (EGFR TKIs), first-generation EGFR TKIs (as gefitinib and erlotinib) are currently used as the front-line standard therapy in treating NSCLC patients with sensitizing EGFR mutations (**Figure 1**) [10]. Nevertheless, despite achieving initial promising clinical responses, most EGFR TKIs-treated patients eventually relapse and progress secondary or acquired resistance.

Cancer cells can develop resistance to EGFR TKIs through adopting several mechanisms that can be classified into three categories; (1) resistance mechanisms involving alterations in the primary drug target (EGFR), (2) alterations in the downstream signaling pathways, (3) or bypass mechanisms employing other RTKs to compensate for EGFR blockade [11]. The most prevalent acquired resistance mechanism is the EGFR mutation T790M, accounting for 50-60% of the cases [12]. The second most frequent mechanism is HER2 amplification as a bypass mechanism that accounts for around 12% of the cases [13]. Hence, there is ultimate need for developing novel EGFR inhibitors to overcome the untiring resistance emerged against the currently used ones. Premised on these findings, we proposed that developing inhibitors that can dually inhibit EGFR and HER2 and can overcome EGFR-T790M mutation as well might overwhelm the development of resistance, and consequently provide better treatment options.

Herein, we present the development of thieno[2,3-*d*]pyrimidine-based dual EGFR/HER2 inhibitors with improved anticancer activities. Two screening cycles led to the identification of **27b** with potent dual EGFR/HER2 inhibitory activity and improved cytotoxicity against diverse patient-derived cancer cells preferentially overexpressing EGFR or HER2 (A431, MDA-MB361 and SKBr3) as well as lapatinib-resistant human NSCLC (NCI-H1975) cell line harboring the T790M mutation.

Figure 1 FDA-approved EGFR inhibitors

2. Rationale and Design

In addition to overcoming the bypass resistance mechanism of HER2 amplification, dual EGFR/HER2 inhibition is proposed to potentiate EGFR pathway blockade and to enhance the anticancer activity for the following reasons [14];

(1) HER2, which has no known ligands, is the favored dimerization partner for the activation of other members of the EGFR family. [15]

(2) HER2-containing heterodimers are more stable with prolonged and enhanced signaling potential. Those heterodimers demonstrate sluggish ligand dissociation, delayed endocytosis, diminished EGFR degradation and rapid receptor recycling [15–17], therefore HER2 overexpression usually predicts poor prognosis [5,16].

Based on these benefits, lapatinib (**Figure 1**) was developed to be the first FDA-approved reversible dual EGFR/HER2 inhibitor indicated for advanced and metastatic breast cancer [18], however, resistance to lapatinib soon developed [19]. Subsequently, Afatinib (**Figure 1**), an irreversible dual EGFR/HER2 inhibitor, was approved for metastatic NSCLC [20], which also encountered acquired resistance through the progression of T790M mutation [21–23], hence the need to develop novel dual EGFR/HER2 inhibitors that can combat resistance.

Our design of dual EGFR/HER2 inhibitors was based on the binding mode of lapatinib in the ATP binding site of EGFR (**Figure 2**). It is assumed that lapatinib adopts a very similar binding mode in HER2 kinase domain owing to the high sequence homology of the two kinase domains (≈80%) [24,25] and the binding mode observed for other dual

inhibitors in both binding sites [26], however, small, yet critical, differences in the sequence of the amino acids in the αC-helix of both enzymes attenuate the stability of the active conformation of HER2 kinase domain compared to that of EGFR, which in turn render the αC-helix of HER2 more flexible with higher accessibility to the back pocket [26], therefore, dual EGFR/HER2 inhibitory activity mostly requires bulky 4-anilino derivatives that can extend into the back pocket [27,28].

Based on the analysis of the binding site (**Figure 2** and **Figure 3**), our approach to design dual EGFR/HER2 inhibitors with the potential to overcome resistance was as follows;

(1) The main mechanism by which T790M mutation causes resistance to the EGFR inhibitors is through increasing the receptor's affinity to ATP with respect to the tyrosine kinase inhibitors [29,30]. Therefore, we proposed increasing the affinity of the inhibitors to the binding site by using the 6-phenylthieno[2,3-*d*]pyrimidine as a core scaffold and a hinge binder. The phenylthiophene is assumed to bind in the hydrophobic pocket II fulfilling the hydrophobic interactions with the surrounding residues (**Figure 4**), the increased hydrophobicity of the phenylthiophene compared to the corresponding phenylfuran in lapatinib is hypothesized to increase the ligand affinity through strengthening the hydrophobic interactions contributing to the enthalpic component of the binding free energy, in addition to an entropic contribution through its favorable desolvation effect [31]. Meanwhile, the N-1 of the pyrimidine is proposed to interact with Met793/EGFR or Met801/HER2 of the hinge region through hydrogen bonds, and N-3 is expected to form a water-mediated hydrogen bond with Thr854/EGFR or Thr862/HER2 (**Figure 4**).

(2) In order to identify the optimum 4-anilino derivative that can fit into the back pocket of EGFR and HER2 and attain desirable dual inhibitory activity *in vitro* and *in vivo*, we constructed and screened a small targeted library of aniline derivatives (**Figure 5**) that were selected based on the review of the literature of the reported dual EGFR/HER2 inhibitors [11].

(3) Finally, with the aim of optimizing the dual inhibitory activity and the pharmacokinetic profile of the elected compound from the first screening cycle, we assembled and screened a small library of solubilizing groups (**Figure 5**) employing variable functionalities (such as amide, sulfonamide, carbamate, urea and Michael acceptor moieties).
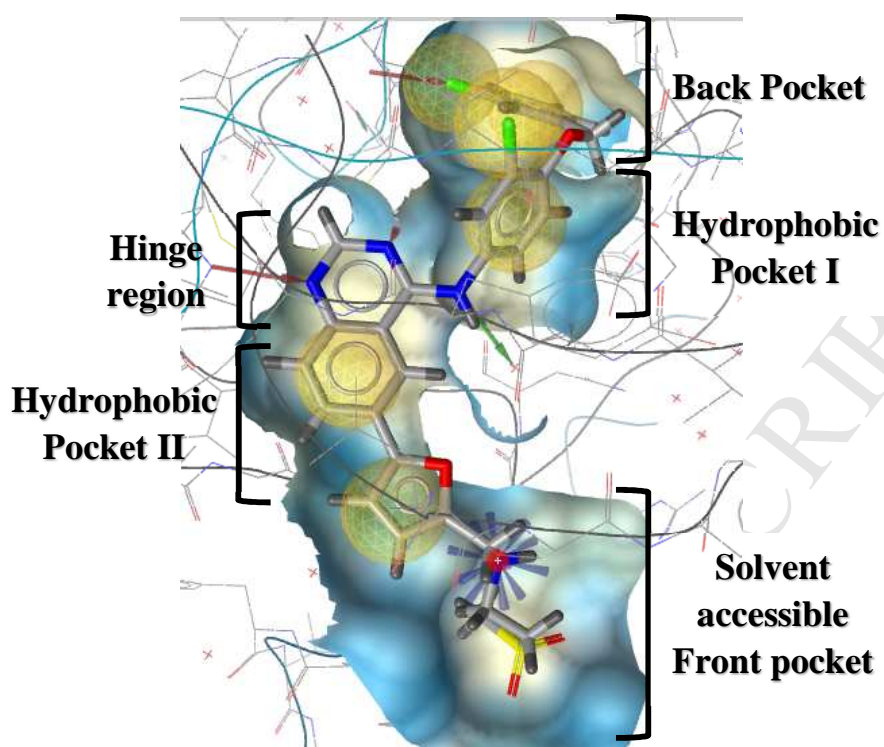
Figure 2 Binding mode of lapatinib in the ATP binding site in the kinase domain of EGFR (PDB: 1XKK). Interactions are illustrated as follows; red arrow= hydrogen bond acceptor, green arrow= hydrogen bond donor, yellow spheres= hydrophobic interactions. The pharmacophore model was generated by LigandScout 4.2.
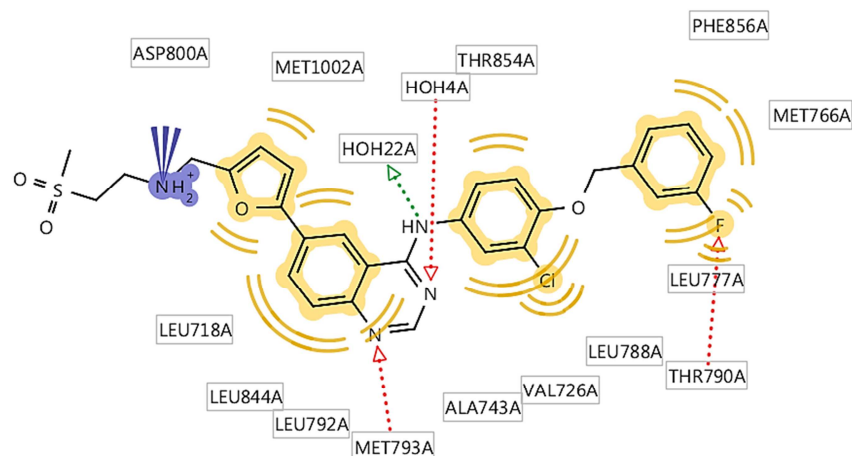
Figure 3 2D interaction diagram of lapatinib in the ATP binding site in the kinase domain of EGFR (PDB: 1XKK) showing the interacting amino acids. Interactions are illustrated as follows; red arrow= hydrogen bond acceptor, green arrow= hydrogen bond donor, yellow highlights= hydrophobic interactions. The diagram was generated by LigandScout 4.2.

Figure 4 Design of thieno[2,3-*d*]pyrimidine-based dual EGFR/HER2 inhibitors

Figure 5 Screening approach for the identification of dual inhibitors. R^1= Library of selected anilines. R^2= Library of selected solubilizing groups. Groups in red have Michael acceptor functionality for the design of irreversible inhibitors.
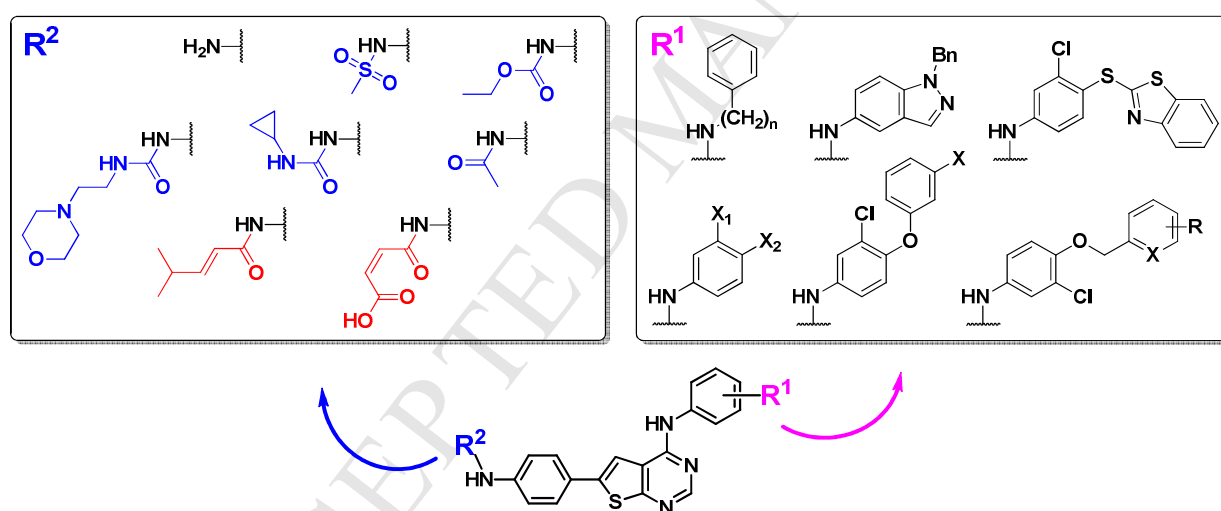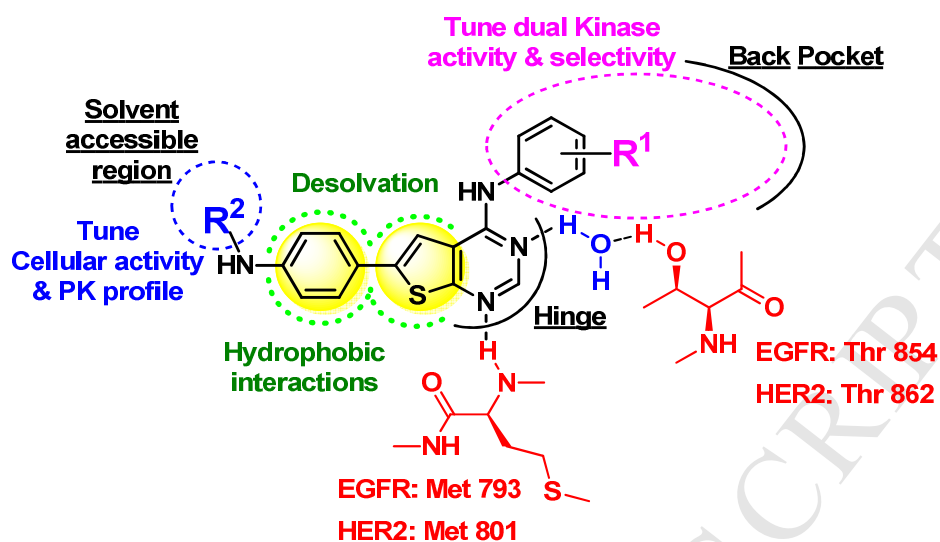
3. Results and Discussion

3.1. Chemistry

The construction of the targeted library of aniline derivatives (R[1]) is outlined in **scheme S1** (see **supplementary**). The benzyloxyaniline derivatives (**2a-d**) (**Scheme S1a**), the phenoxyaniline derivatives (**4a,b**) (**Scheme S1b**) and the 1-benzyl-1*H*-indazol-5-amine (**6**) (**Scheme S1c**) were prepared following similar previously reported procedures (**2a-d** [32,33], **4a,b** [34,35], **6** [36]). The 4-(benzo[*d*]thiazol-2-ylthio)-3-chloroaniline (**8**) was prepared through a nucleophilic aromatic substitution (S_NAr) between 2-chloro-1-fluoro-4-nitrobenzene and benzo[*d*]thiazole-2-thiol by heating in presence of potassium carbonate in dimethylformamide, followed by the reduction of the nitro derivative (**7**) with stannous chloride dihydrate in ethyl acetate.

The synthetic route for the preparation of the target compounds (**13-20**) for the first screening cycle is shown in **scheme 1**. Firstly, the core scaffold, 4-chloro-6-(4-nitrophenyl)thieno[2,3-*d*]pyrimidine (**12**), was synthesized starting with a Batcho-Leimgruber-like condensation between 4-nitrotoluene and *N,N*-dimethylformamide dimethyl acetal in dimethylformamide affording the enamine (**9**) [37], followed by Gewald's 2-aminothiophene synthesis through a one-pot reaction between the enamine (**9**), ethyl cyanoacetate, elemental sulfur and morpholine in ethanol giving the 2-aminothiophene (**10**) [38] which was then cyclized by heating with formamide into the thieno[2,3-*d*]pyrimidinone (**11**), eventually, (**11**) was activated for nucleophilic substitution by chlorination with phosphorus oxychloride producing the activated 4-chloro-6-(4-nitrophenyl)thieno[2,3-*d*]pyrimidine (**12**). Subsequently, the target compounds (**13-18**) were obtained by nucleophilic substitution of the 4-chloro derivative (**12**) with varied aniline derivatives (R[1]) in i-propanol or n-butanol.

With the aim of further optimization of the solubilizing group, compounds **14a**, **17a** and **18a** were reduced into their corresponding aniline derivatives **21**, **19** and **20**, respectively, using iron and ammonium chloride in ethanol/water.

Finally, varied solubilizing groups (R[2]) were installed in compounds **21**-**27** following the synthetic pathways illustrated in **scheme 2**.
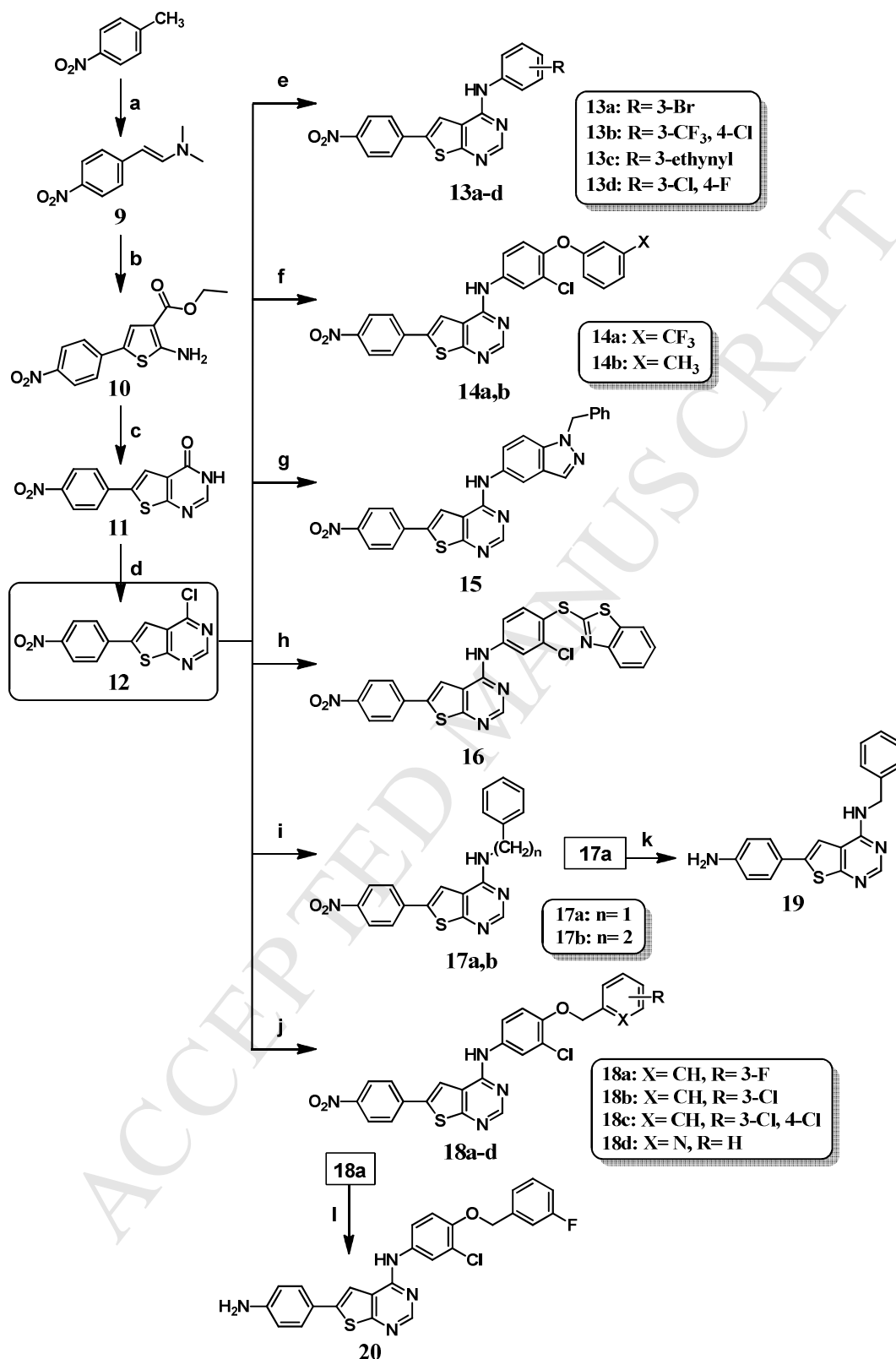
Scheme 1. Synthesis of Compounds **13-20**

Reagents and Conditions: **(a)** DMF-DMA, DMF, 110 °C, 48 h, 70%, **(b)** Ethyl cyanoacetate, Sulfur powder, morpholine, EtOH, reflux 24 h, 85%, **(c)** Formamide, 200 °C, 5 h, 90%, **(d)** POCl$_3$, reflux 24 h, 50%, **(e)** aniline derivatives, i-propanol, reflux 24-72h, 20-80%, **(f) 4a,b**, n-butanol, reflux 24 h, 32-54%, **(g) 6**, i-propanol, reflux 48 h, 40%, **(h) 8**, i-propanol, reflux 72 h, 43%, **(i)** amine, i-propanol, reflux 24-48 h, 53-80%, **(j) 2a-d**, n-butanol, reflux 24-48 h, 25-41%, **(k)** Fe, NH$_4$Cl, EtOH, H$_2$O, reflux 3 h, 20%, **(l)** Fe, NH$_4$Cl, EtOH, H$_2$O, reflux 2 h, 100%.
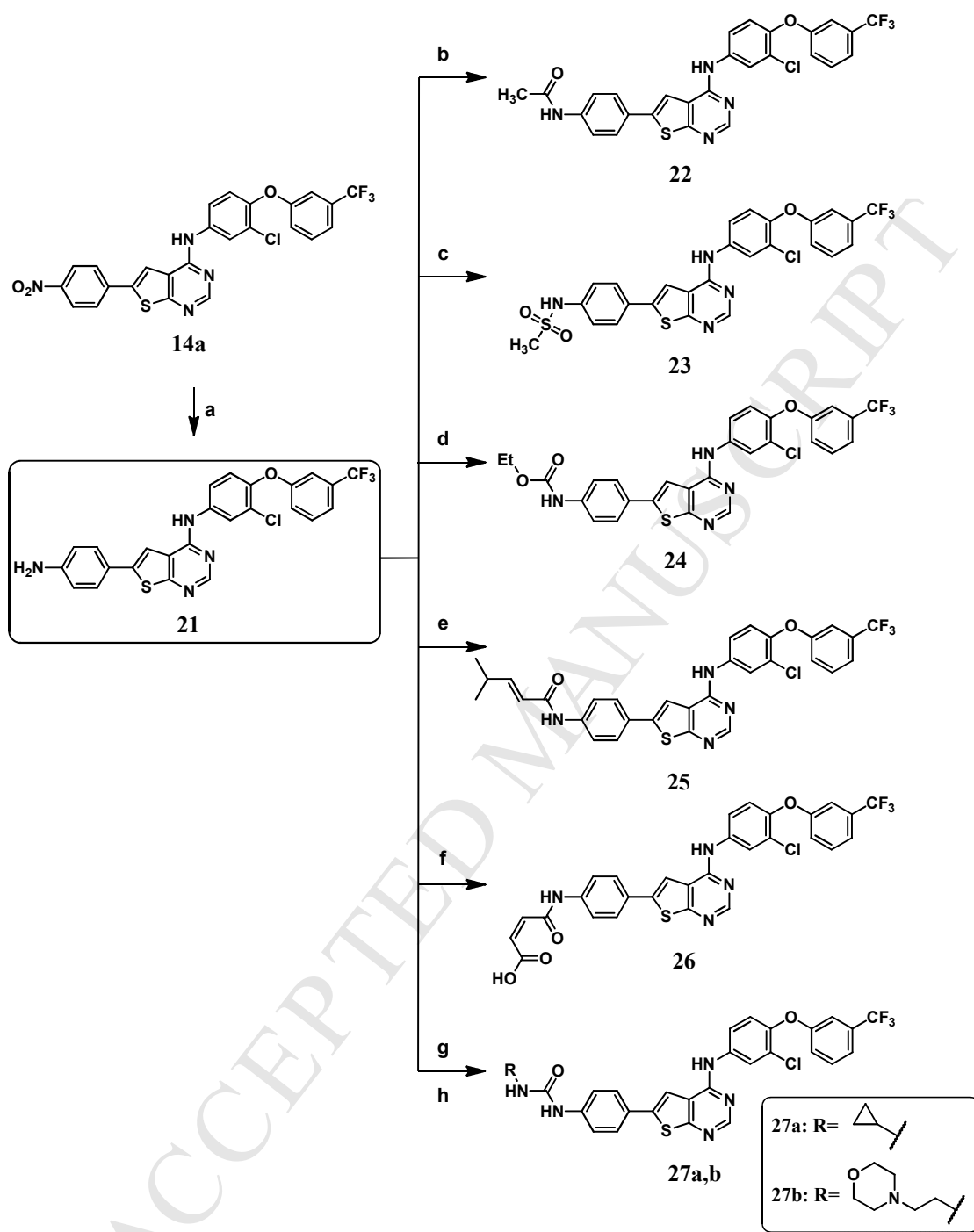
Scheme 2. Synthesis of Compounds **21**-**27**

Reagents and Conditions: **(a)** Fe, NH$_4$Cl, EtOH, H$_2$O, reflux 2 h, 100%, **(b)** Acetic anhydride, THF, rt, 24 h, 35%, **(c)** Methanesulfonyl chloride, pyridine, rt, 24 h, 35%, **(d)** Ethyl chloroformate, pyridine, rt, 24 h, 40%, **(e)** 4-methyl-pent-2-enoic acid, EDC.HCl, DMAP, DMF, rt, 24 h, 10%, **(f)** Maleic anhydride, THF, rt, 24 h, 59%, **(g)** Triphosgene, THF, reflux 4 h, **(h)** amine, THF, reflux 24 h, 35%.

3.2. Screening cycle (1): identifying the aniline derivative

3.2.1. *In vitro* EGFR/HER2 kinase inhibitory activity at 10 μM

In order to identify the aniline derivative that can afford dual inhibitory activity, compounds **13**-**18** – bearing variable 4-anilino derivatives – were preliminary screened for their dual inhibitory activity through determining their % inhibition at 10 μM against EGFR and HER2. Based on the results shown in **Table 1**, the compounds were categorized into four groups that reflect certain structure-activity relationships (SAR) for the R^1 moiety:

(a) ***Compounds with good EGFR inhibition (80-86%) & good HER2 inhibition (63-72%):*** compounds **14a**, **15**, **18a** and **18d** showed good dual inhibitory activities of 80%, 85%, 86% and 82% against EGFR, respectively, and 67%, 63%, 72% and 65% against HER2, respectively. It can be observed that all these compounds are bearing bulky aniline headgroups (R^1), that are capable of extending into the back pocket such as phenoxyaniline (**14a**), *N*-benzyl indazole (**15**) and benzyloxyanilines (**18a,d**), conforming to the reported SAR of dual inhibitors [27,28].

(b) ***Compounds with moderate EGFR inhibition (67-81%) & moderate HER2 inhibition (46-56%):*** compounds **14b**, **17a**, **17b** and **18b** showed moderate dual inhibitory activities of 81%, 76%, 67% and 70% against EGFR, respectively, and 51%, 56%, 46% and 43% against HER2, respectively. Compounds **14b** and **18b**, though they are structurally-related to compounds **14a** and **18a** with the same bulky headgroups, showed weaker dual inhibitory activities than their respective analogues. This discrepancy in activities can be attributed to the only structural variability which is the substituent at the 3' position. It can be inferred that the presence of a fluoro substituent at the 3' position – 3'-CF$_3$ in **14a** opposite to 3'-CH$_3$ in **14b** and 3'-F in **18a** opposite to 3'-Cl in **18b** – greatly enhanced the dual inhibitory activity which might be attributed to the extra hydrogen bonding that fluoro can establish with the gatekeeper in the back pocket (Thr790/EGFR or Thr798/HER2) (**Figure 3**) [39]. As for compounds **17a** and **17b** bearing the aromatic amines (benzylamine for **17a** and phenethylamine for **17b**), they also demonstrated moderate dual inhibitory activities despite having much less bulkier headgroups.

(c) ***Compounds with good EGFR inhibition (68-87%) & poor HER2 inhibition (19-35%):*** compounds **13a**, **13c** and **13d** showed selectivity towards EGFR with good EGFR inhibitory activities of 86%, 87% and 68%, respectively, while showing poor HER2 inhibitory activities of 28%, 35% and 19%, respectively. Also conforming to the SAR of dual inhibitors, these compounds bearing simple monocyclic anilines failed to maintain activity against HER2, emphasizing the importance of back pocket-binding in order to attain HER2 activity.

(d) ***Compounds with poor EGFR inhibition (18-21%) & poor HER2 inhibition (8-16%):*** compounds **13b**, **16** and **18c** showed poor activities towards both enzymes of 18%, 18% and 21% against EGFR, respectively, and 8%, 10% and 16% against HER2, respectively.

Firstly, compound **13b** showed very poor activities albeit carrying a simple monocyclic aniline like **13a,c,d**. Attempting to explain its inactivity would require us to draw a comparison between the structures of the four structurally-related compounds (**13a-d**). The main difference between the four anilines is the substituent at the 3 position. The three EGFR-active compounds have 3-Br (**13a**), 3-ethynyl (**13c**) and 3-Cl (**13d**), while the inactive one has a 3-CF$_3$ (**13b**). A common factor between the three active moieties which doesn't apply to the inactive one is their abilities to form halogen bonds. Br and Cl (especially when associated with an electron-withdrawing group like the 4-F in **13d**) are capable of forming halogen bonds while F can't [40]. The ethynyl group (as a 'supramolecular halogen' [41]) is capable of forming a hydrogen bond equivalent to the halogen bond [42]. Based on these assumptions, we can hypothesize that the activity against EGFR requires the formation of a halogen bond in the hydrophobic pocket I.

Compound **16** with the 4-(benzo[*d*]thiazol-2-ylthio)-3-chloroaniline also showed very poor activity against both enzymes despite having a bulky aniline resembling the active phenoxyaniline derivatives (**14a,b**). This might be attributed to the difference between the biaryl ethers (**14a,b**) and the thioether (**16**) in the bond angles between the linker atom and the biaryl substituents. C-S-C angle approaches 90°, while the C-O-C angle is approximately 110° [43], therefore, the conformation of the benzothiazolylthioaniline must be different from that of the phenoxyaniline, and the sulfur linker might be bringing the second ring into clash with the gatekeeper residue hindering it from properly extending into the back pocket.

Finally, the inactivity of the benzyloxyaniline-bearing compound **18c** was quite surprising compared to the activities of the other benzyloxyaniline analogues **18a,b,d**. It seems that the additional 4'-Cl abolished the activity which can be ascribed to a steric clash with the binding site arose by the extra 4'-substituent.

Based on these results, compounds **14a**, **15**, **18a** and **17a** were selected for further anticancer activity testing. These were the most active representatives from the four classes of dually active compounds determined during this screening (**14a** for phenoxyanilines, **15** for *N*-benzyl indazole, **18a** for benzyloxyanilines and **17a** for aromatic amines).

3.2.2. *In vitro* antiproliferative activity against A431 and MDA-MB-361 cancer cell lines

The anticancer activities of these compounds were further tested using the SRB cytotoxicity assay on patient-derived epidermoid (A431) and breast (MDA-MB-361) cancer cell lines which overexpress EGFR and HER2, respectively [44]. Lapatinib was used as a reference compound. As shown in **Table 1**, compound **14a** evidently reduced the viability of A431 cells with IC_{50} of 1.72 μM which was comparable to that of lapatinib (1.69 μM). Also, in alignment with the inhibitory effects on HER2, compounds **14a** and **18a** exhibited more potent cytotoxicity against MDA-MB-361 cells (with IC_{50} values of 3.65 and 7.5 μM, respectively) compared to lapatinib (IC_{50} = 13.73 μM). Compound **15** showed minimal potency as an antiproliferative agent against A431 and MDA-MB-361 cells though it exhibited appreciated inhibitory effects on EGFR and HER2 assay *in vitro*. This could be secondary to reduced cellular uptake of this compound. Compound **17a** on the other hand demonstrated more notable cytotoxicity against A431 cells than **18a**, though not as potent as **14a**, while showed minimal activity against MDA-MB-361 cells.

3.2.3. Reduction of the nitro group (R^2)

Emerging from the previous results, we selected compounds **14a**, **17a** and **18a** for further optimization. With the aim of improving the kinase inhibitory activity of the compounds, the reduction of the nitro group at the solubilizing group position (R^2) into the corresponding NH_2 derivative was sought. The nitro group, albeit highly polar, is considered to be "hydroneutral" rather than being hydrophilic [45], and since the solubilizing group extends into the solvent accessible front pocket, we proposed that a more hydrophilic moiety (such as the NH_2 group) would offer a better physicochemical complementarity.
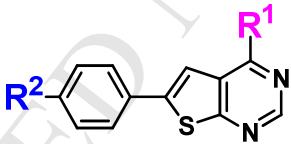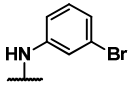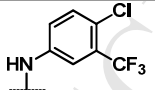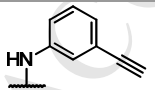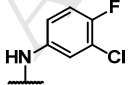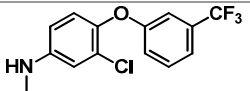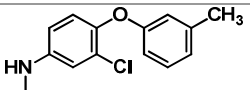
As presented in **Table 1**, transforming the R^2 from NO_2 (in compounds **14a**, **17a** and **18a**) into the more hydrophilic NH_2 (compounds **21**, **19** and **20**, respectively) dramatically improved the dual kinase inhibitory activities of the compounds with a more pronounced effect on their HER2 activities, for instance, **19** exhibited superior dual inhibitory activities of 99% (EGFR) and 96% (HER2) compared to its NO_2 parent, **17a**, that displayed activities of 76% (EGFR) and 56% (HER2), and similar patterns were observed for **20** (HER2; 90% versus 72% for **18a**) and **21** (97% and 96% versus 80% and 67% of **14a** against EGFR and HER2, respectively). These observations accentuate the influence of optimizing the solubilizing group on the kinase inhibitory activity. Moreover, compounds **18a** (NSC: D-793249/1) and its aniline derivative **20** (NSC: D-793254/1) were submitted to the Developmental Therapeutics Program (DTP) of the National Cancer Institute (NCI) for screening against the NCI-60 panel of human cancer cell lines. The two compounds were tested at an initial 1-dose (10 μM) assay determining the growth percent of the full NCI-60 panel. The results of the assay (**Supplementary Figures S2, S3**) illustrate an overall enhancement of cytotoxicity upon reducing the NO_2

(**18a**) into NH$_2$ (**20**) subsiding from a mean growth percent of 79% (**18a**) to 42% (**20**). Focusing on the lapatinib-sensitive cell lines [46] (listed in **Table 2**), we can notice a consistent improvement in the cytotoxicity of **20** against these particular cell lines compared to **18a** (**Table 2**), again affirming the significance of optimizing the hydrophilicity of the solubilizing group for dual inhibitory activity.
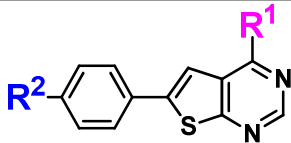
Finally, the cytotoxicity of the three compounds (**19**, **20** and **21**) against A431 and MDA-MB-361 cell lines was determined. In contrast to their kinase inhibitory effects, compounds **19** and **21** exhibited anticancer activities inferior to their respective NO$_2$ parents (**17a** and **14a**). This highlights the need to further optimize the solubilizing group – balancing its hydrophilicity and the overall polarity of the compound – in order to attain optimum cellular activities. While compounds **20** and **21** showed comparable cytotoxic activities, compound **21** was selected for optimization through the second screening cycle since its aniline headgroup (3-chloro-4-(3-(trifluoromethyl)phenoxy)aniline) was previously identified through a fragment-based drug design approach as being effective against EGFR-T790M [47].

Table 1 % inhibitory effect on EGFR/HER2 kinase activities at 10 μM and anticancer activity against A431 and MDA-MB-361 of compounds **13-21**

Comp	R^1	R^2	% inhibition at 10 μM		Cytotoxicity (IC$_{50}$)* – μM	
			EGFR	HER2	A431	MDA-MB-361
13a		NO$_2$	86	28	---	---
13b		NO$_2$	18	8	---	---
13c		NO$_2$	87	35	---	---
13d		NO$_2$	68	19	---	---
14a		NO$_2$	80	67	1.72 ± 0.03	3.65 ± 1.62
14b		NO$_2$	81	51	---	---

Comp	R^1	R^2	% inhibition at 10 μM		Cytotoxicity (IC$_{50}$)* – μM	
			EGFR	HER2	A431	MDA-MB-361
15		NO$_2$	85	63	>20	>20
16		NO$_2$	18	10	---	---
17a		NO$_2$	76	56	4.87 ± 0.17	>20
17b		NO$_2$	67	46	---	---
18a		NO$_2$	86	72	11.00 ± 0.98	7.50 ± 2.94
18b		NO$_2$	70	43	---	---
18c		NO$_2$	21	16	---	---
18d		NO$_2$	82	65	---	---
19		NH$_2$	99	96	>20	>20
20		NH$_2$	87	90	9.76 ± 1.18	5.70 ± 0.53
21		NH$_2$	97	96	11.37 ± 2.20	5.85 ± 0.90

			% inhibition at 10 μM		Cytotoxicity (IC$_{50}$)* – μM	
Comp	**R^1**	**R^2**	**EGFR**	**HER2**	**A431**	**MDA-MB-361**
Staurosporine (1 μM)			86%	94%	---	---
Lapatinib di-p-toluenesulfonate			---	---	1.69 ± 0.26	13.73 ± 2.32

* IC$_{50}$ values are expressed as mean ± SD and were obtained using Graphpad prism software based on the data obtained from triplicates of at least two independent experiments

Table 2 % inhibition of **18a** and **20** at 10 μM against selected NCI-60 cancer cell lines

Lapatinib-sensitive cancer cell lines [46]	% inhibition* of **18a** at 10 μM against the selected cell lines	% inhibition* of **20** at 10 μM against the selected cell lines
Lung EKVX	20%	80%
Lung NCI-H322M	15%	75%
Ovarian IGROV1	12%	60%
Ovarian SK-OV-3	0%	100%
Renal ACHN	23%	70%
Renal TK-10	30%	70%
Breast MDA-MB-468	40%	85%

* Approximated values calculated from the growth percent values shown in the one dose mean graph provided by NCI-developmental therapeutics program (**Supplementary Figures S2, S3**)

3.3. Screening cycle (2): optimizing the solubilizing group

3.3.1. *In vitro* EGFR/HER2 kinase inhibitory activity at 10 μM

During the second screening cycle, we were on a quest to find the solubilizing group that could afford the desirable balance between the required hydrophilicity for optimum kinase activity and the hydrophobicity needed for cellular permeability. Deriving from compound **21**, a series of compounds (**22-27**) decorated with varied solubilizing groups (R^2) was synthesized and their kinase inhibitory activities at 10 μM were determined (**Table 3**). Compounds **26** and **27b** maintained inhibitory activities comparable to **21**, while **22** and **23** only exhibited similarly potent EGFR inhibition (98% and 92%,

respectively) and much less potent HER2 inhibition (74% and 65%, respectively). Finally, **24**, **25** and **27a** showed reduced dual inhibitory activities compared to **21** with a more prominent decline in HER2 inhibition (52%, 46% and 44%, respectively). One factor that might be contributing to this pattern of activity is the hydrophilicity of the solubilizing group. Evidently the solubilizing groups of compounds **24**, **25** and **27a** have the highest logP values in this series (**Supplementary Table S1**), and so they showed the least potent HER2 activities, while **26** and **27b** have lower logP values closer to **21**, hence their potent HER2 inhibitory activities. Apparently HER2 inhibition, and accordingly dual inhibition, requires certain hydrophilicity in the solubilizing group.

3.3.2. *In vitro* antiproliferative activity against A431 and MDA-MB-361 cancer cell lines

Like the first series of compounds, the anticancer activities of the second series of compounds were also determined using SRB cytotoxicity assay on A431 and MDA-MB-361 cancer cell lines. As demonstrated in **Table 3**, compounds **27a** and **27b** diminished A431 viability with IC_{50} values of 2.34 and 1.45 μM, respectively, which were comparable to that of lapatinib. Additionally, they exhibited superior antiproliferative activities on MDA-MB-361 cells as compared to lapatinib with IC_{50} values of 3.83 and 3.5 μM, respectively. The strong anticancer activities of compound **27a** on A431 and MDA-MB-361 cells are inconsistent with its kinase assay data. This could be due to the inhibitory effects of compound **27a** on other crucial prosurvival signalling kinases involved in A431 and MDA-MB-361 proliferation, since the cyclopropyl urea moiety is reported to be encountered in other kinase inhibitors (like the multikinase inhibitor lenvatinib, or the Aurora kinase inhibitor AT9283) [48]. Not only did the cytotoxicity of **27b** conform to its kinase inhibition, but also in alignment with its evident antiproliferative activity on MDA-MB-361 cells, **27b** induced apoptotic cell death in those cells in a concentration-dependent pattern as illustrated by Annexin V/PI staining (**Figure 6**). Interestingly, compound **25** demonstrated remarkable antiproliferative activity on A431 cells compared to lapatinib with IC_{50} value of 0.23 μM, while showed minimal activity against MDA-MB-361 cells (IC_{50} >20 μM). Compounds **22** and **23** showed dual cellular inhibition though with lower potencies on A431 compared to lapatinib with IC_{50} values of 10.5 and 5.25 μM, respectively. Consistently, compounds **21**, **22** and **27b** significantly decreased the proliferation of SKBr3 - another human breast cancer cell line which overexpresses HER2 [44] - with IC_{50} values of 6, 4.7 and 4.83 μM respectively (**Table 5**). Despite its potent kinase inhibitory activities, compound **26** showed negligible antiproliferative activities against A431 and MDA-MB-361 cells, this might be attributed to its high polarity hampering its cell permeability. Finally, compound **24** showed minimal cytotoxicity against both cancer cell lines even though it exhibited appreciated

inhibitory effects on EGFR and HER2 which could also be ascribed to the reduced cellular uptake of this compound.
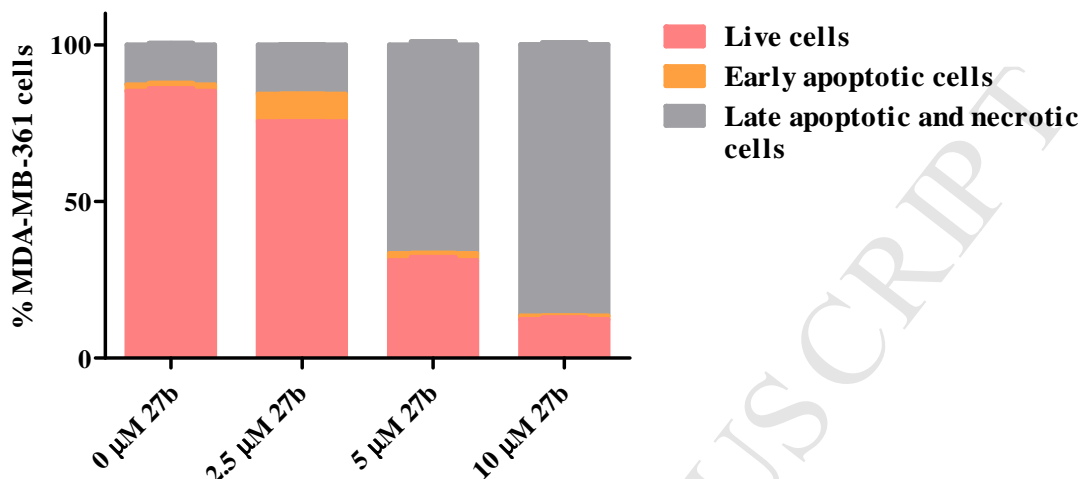
Figure 6 Compound 27b induces apoptosis in human breast cancer (MDA-MB-361) cells. Twenty four hours after treatment with **27b**, MDA-MB-361 cells were subjected to Annexin V/PI staining and percent of live cells, early as well as late apoptotic and necrotic cells were analysed using flow cytometry.

3.3.3. Potential EGFR/HER2 kinase inhibitory activity (IC_{50}) determination

Hinging upon the previous assays, five compounds (**21**, **22**, **23**, **27a** and **27b**) that maintained dual inhibitory activities both enzymatically and cellular were selected for kinase IC_{50} determination. Their dose-related EGFR/HER2 inhibition at 5 concentrations (1 nM, 10 nM, 100 nM, 1 μM and 10 μM) were measured in order to determine their IC_{50} values. The five compounds showed EGFR IC_{50} in the nanomolar range, and HER2 IC_{50} in low to sub-micromolar range (**Table 4**), except for the two compounds **23** and **27a** that exhibited less potent HER2 inhibition with IC_{50} values >20 μM. Eventually, the three compounds **21**, **22** and **27b** were identified as potent dual EGFR/HER2 inhibitors with good cytotoxic activities against cancer cell lines overexpressing EGFR and/or HER2, representing promising candidates.

3.3.4. Inhibitory activities of tested compounds on EGFR/HER2 signaling in human cancer cells

In addition to the kinase inhibitory and anticancer activities of the tested compounds, we further evaluated whether these compounds could inhibit EGFR/HER2 signalling pathways in A431 and SKBr3 cells which overexpress EGFR and HER2, respectively. Compounds **21**, **22** and **27b** were selected for further experiments. A431 cells were serum starved overnight and then incubated with varying concentrations of **21** and **27b** for 3h

before being stimulated with EGF. Potent and concentration-dependent inhibition of phosphorylation of EGFR was observed after treatment with **21** and **27b** (**Figure 7**). Moreover, **21** and **27b** evidently inhibited EGF-induced activation of downstream signalling effectors as shown by reduced phosphorylation of AKT, p70 S6 kinase and ribosomal S6 (**Figure 7**). Furthermore, **22** inactivated AKT/mTOR/S6 signalling in HER2 overexpressing SKBr3 cells (**Figure 8**).
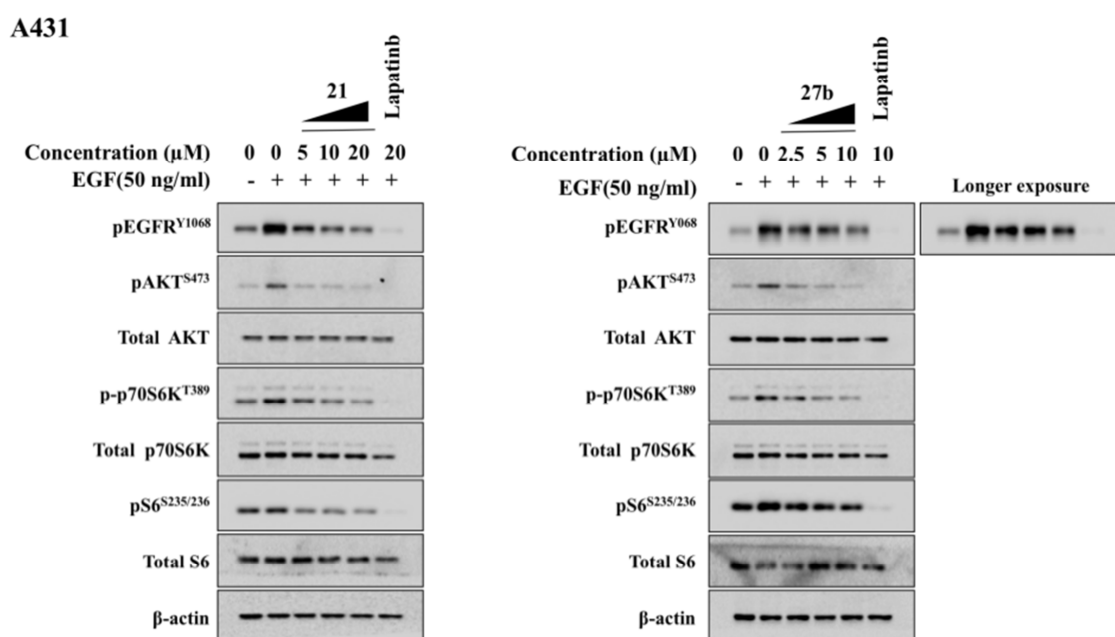
Figure 7 Effect of compounds 21 and 27b on EGF-induced EGFR phosphorylation in EGFR overexpressing human epidermoid carcinoma (A431) cells. A431 cells were serum-starved overnight and then treated with the indicated concentrations of compounds **21** and **27b** for 3h before being stimulated with EGF for 10 min. Representative western blot analysis of inhibition of EGFR and its downstream targets by **21** and **27b** in A431 cell line. β-actin served as the loading control.
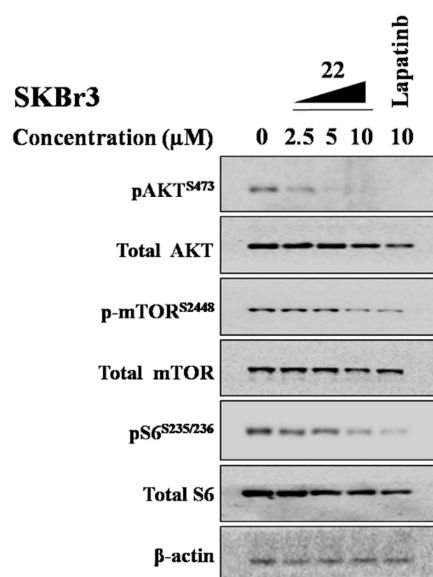
Figure 8 Effect of compound 22 on AKT/mTOR/S6 signalling pathway in HER2 overexpressing human breast cancer (SKBr3) cells. Representative western blot analysis of AKT/mTOR/S6 signalling in cell lysates of SKBr3 treated with the indicated concentrations of **22** for 72h. β-actin served as the loading control.

3.3.5. Inhibition of EGFR signaling in lapatinib-resistant non-small lung cancer (NCI-H1975) cells harboring T790M mutation

Drug resistance is a critical and frequently encountered issue in cancer therapy, and T790M mutation in EGFR has been reported to contribute to lapatinib, gefitinib and erlotinib resistance [29]. Hence, development of novel EGFR inhibitors is ultimately needed. We then questioned whether these compounds could inhibit the growth of human non-small lung cancer cells (NCI-H1975) which harbour EGFR T790M mutation. Intriguingly, compound **27b** dramatically impeded NCI-H1975 proliferation with IC_{50} value of 4.2 μM (**Figure 9A and Table 5**) and increased % of apoptotic and necrotic cells in NCI-H1975-treated cells (**Figure 9B**).
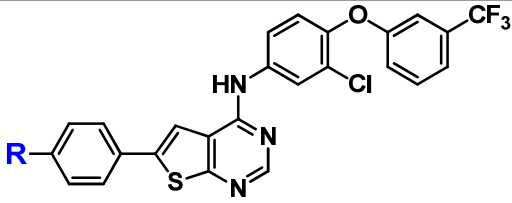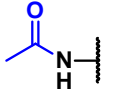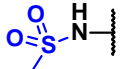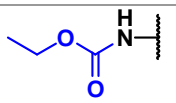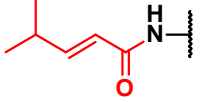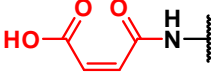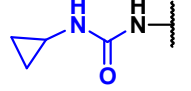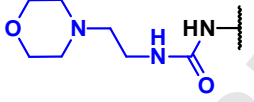
We then examined the ability of compound **27b** to inhibit EGFR T790M signalling pathway in NCI-H1975 cells. Indeed, compound **27b** robustly inactivated AKT/S6K/S6 signalling in treated NCI-H1975 cells in a concentration-dependent pattern (**Figure 9C**). In addition, compound **27b** thwarted EGF-induced activation of EGFR and its downstream signalling molecules including AKT, p70 S6 kinase and ribosomal S6 in NCI-H1975 cells which were serum starved overnight and then incubated with compound **27b** for 2.5 h followed by EGF stimulation (**Supplementary Figure S4**).
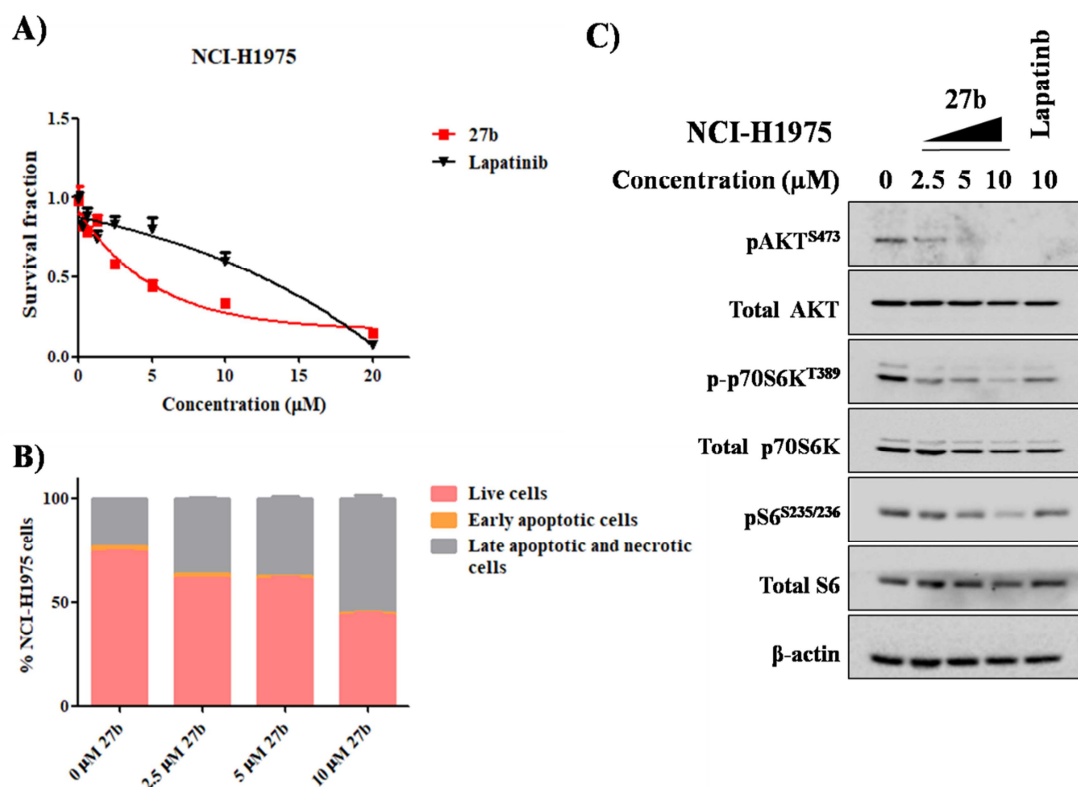
Figure 9 Apoptotic effects of compound 27b in human non-small cell lung carcinoma (NCI-H1975) cells harbouring T790M mutation are associated with inhibition of EGFR downstream signalling effectors (AKT/S6K/S6). A) Anticancer activity of compound **27b** against NCI-1975 cells following 72h of treatment with the indicated concentrations were assessed using SRB cytotoxicity assay. **B)** Seventy two hours after treatment with **27b**, NCI-H1975 cells were subjected to Annexin V/PI staining and percent of live cells, early as well as late apoptotic and necrotic cells were analysed using flow cytometry. **C)** Representative western blot analysis of AKT/S6K/S6 signalling in cell lysates of NCI-H1975 treated with the indicated concentrations of **27b** for 72h. β-actin was used as the loading control.

Table 3 % inhibitory effect on EGFR/HER2 kinase activities at 10 μM and anticancer activity against A431 and MDA-MB-361 of compounds **22-27**

Comp	R	% inhibition at 10 μM		Cytotoxicity (IC$_{50}$)* – μM	
		EGFR	**HER2**	**A431**	**MDA-MB-361**
22		98	74	10.50 ± 1.41	10.45 ± 3.06
23		92	65	5.25 ± 0.35	9.86 ± 2.74
24		85	52	17.00 ± 0.98	>20
25		81	46	0.23 ± 0.04	>20
26		92	98	>20	>20
27a		76	44	2.34 ± 0.17	3.83 ± 0.23
27b		100	97	1.45 ± 0.21	3.50 ± 0.73
Staurosporine (10 μM)		100%	100%	---	---
Lapatinib di-p-toluenesulfonate		---	---	1.69 ± 0.26	13.73 ± 2.32

* IC$_{50}$ values are expressed as mean ± SD and were obtained using Graphpad prism software based on the data obtained from triplicates of at least two independent experiments

Table 4 IC_{50} values of compounds **21**, **22**, **23**, **27a** and **27b** against EGFR and HER2

Compound ID	EGFR IC_{50} (nM)	HER2 IC_{50} (μM)
21	**21.4 nM**	**1.5 μM**
22	**47.7 nM**	**0.879 μM**
23	**47.1 nM**	**19.2 μM**
27a	**112 nM**	**37.1 μM**
27b	**91.7 nM**	**1.2 μM**
Staurosporine	**47 nM**	**60.8 nM**

Table 5 Anticancer activity of tested compounds (**21**, **22** and **27b**) against SKBr3 and NCI-H1975 cancer cell lines

Compound ID	Cytotoxicity (IC_{50})* – μM	
	SKBr3	**NCI-H1975**
21	6.00 ± 1.10	13.90 ± 2.40
22	4.70 ± 2.08	12.69 ± 3.98
27b	4.83 ± 1.06	4.20 ± 0.19
Lapatinib di-p-toluenesulfonate	0.17 ± 0.04	11.46 ± 2.45

* IC_{50} values are expressed as mean $\pm$ SD and were obtained using Graphpad prism software based on the data obtained from triplicates of at least two independent experiments

3.4. Molecular modeling studies

3.4.1. Molecular docking study

Molecular docking was performed using CDOCKER protocol in Accelrys Discovery Studio® 2.5. This docking study was performed to gain insight into the SAR of the target compounds, and as an attempt to interpret the observed enzymatic activities of the tested compounds on the basis of the ligand-protein interactions. The enzymatic activity of kinase inhibitors depends on the ability of the compound to properly dock into the binding site and to establish strong enough interactions with the key amino acids (ligand affinity) in order to compete with the ATP for the binding site. Accordingly, the active compounds in this study should attain the same binding mode observed for lapatinib (**Figure 2** and **Figure 3**) and kinase inhibitors in general, and to establish the key

interactions with the binding site, while the inactive compounds would fail either to achieve the correct pose and/or to establish the desired interactions. The results of the docking study (**Supplementary Table S2**) will be discussed in order of the activity of the compounds as follows:

- *Compounds with good EGFR inhibition (80-86%) & good HER2 inhibition (63-72%):* compounds **14a**, **15** and **18a** showed the same binding modes as lapatinib in both EGFR (PDB: 3POZ) and HER2 (PDB: 3RCD) (exemplified by the binding modes of compound **21** in **Figure 10** and **Figure 11**), that are also conforming to the proposed binding mode (**Figure 4**), where the hinge binder is correctly positioned in the hinge region properly directing the aniline headgroup into the back pocket and conveniently extending the solubilizing group towards the solvent accessible region. Additionally, the three compounds successfully established all the key interactions with the binding site of EGFR, such as the HB of N1 with the hinge region (Met793), and the HB of N3 through the water bridge, also the π-+ interaction of the aniline ring with the Lys745 that interrupts the salt bridge with the Glu762 and hampers the active protein conformation, in addition to a π-σ interaction between the thiophene ring and Leu718 (hydrophobic region II), also the nitro group formed a charge interaction with the Asp800 in the solvent accessible region. Similar binding modes and interactions were observed in HER2, in addition to the extra HB of the CF_3 (**14a**) and 3-F (**18a**) with the gatekeeper residue Thr798 in the back pocket, which explains their higher activities on HER2 compared to other analogues.

- *Compounds with moderate EGFR inhibition (67-81%) & moderate HER2 inhibition (46-56%):* represented by compound **17a**, the compound showed the same binding mode and interactions in EGFR but it was missing the key HB with Met793, which might explain its lower EGFR activity, while the docking protocol could only generate a flipped pose for the compound in the binding site of HER2 with the amine and the solubilizing groups exchanging positions, which could also be a probable explanation for the lower HER2 inhibition.

- *Compounds with good EGFR inhibition (68-87%) & poor HER2 inhibition (19-35%):* compounds **13a**, **13c** and **13d** achieved similar binding modes and interactions like lapatinib with both EGFR and HER2. Their poor activities on HER2 couldn't be explained through their docking results which seem to be about right, however, in our experience, HER2 inhibitors usually have aniline headgroups extending into the back pocket which they don't have.

- *Compounds with poor EGFR inhibition (18-21%) & poor HER2 inhibition (8-16%):* Unexpectedly, compound **13b** showed the correct pose and the correct interactions in both EGFR and HER2 comparable to the active compounds, however, the docked pose is of a high energy conformer (CHARMm Energy= 9.58482)

(compared to its global minimum conformer with CHARMm Energy of 4.41552), hence its minimal inhibition. Compound **16** showed a skewed pose in EGFR due to the improper fitting of the benzothiazole in the back pocket, so it failed to establish any of the essential interactions, while in HER2 it failed to achieve the correct pose also due to the lower flexibility of the benzothiazolylthioaniline that hinders the proper positioning of the hinge binder and so the remaining moieties. Again, compound **18c** showed the correct pose and all the proper interactions in EGFR though it is inactive on EGFR which might be attributed to that the docked pose is of a high energy conformer (CHARMm Energy= 32.1588) compared to the global minimum with CHARMm Energy of 14.1322. On the other hand, **18c** showed a flipped pose in HER2, failing to achieve the proper pose and interactions.
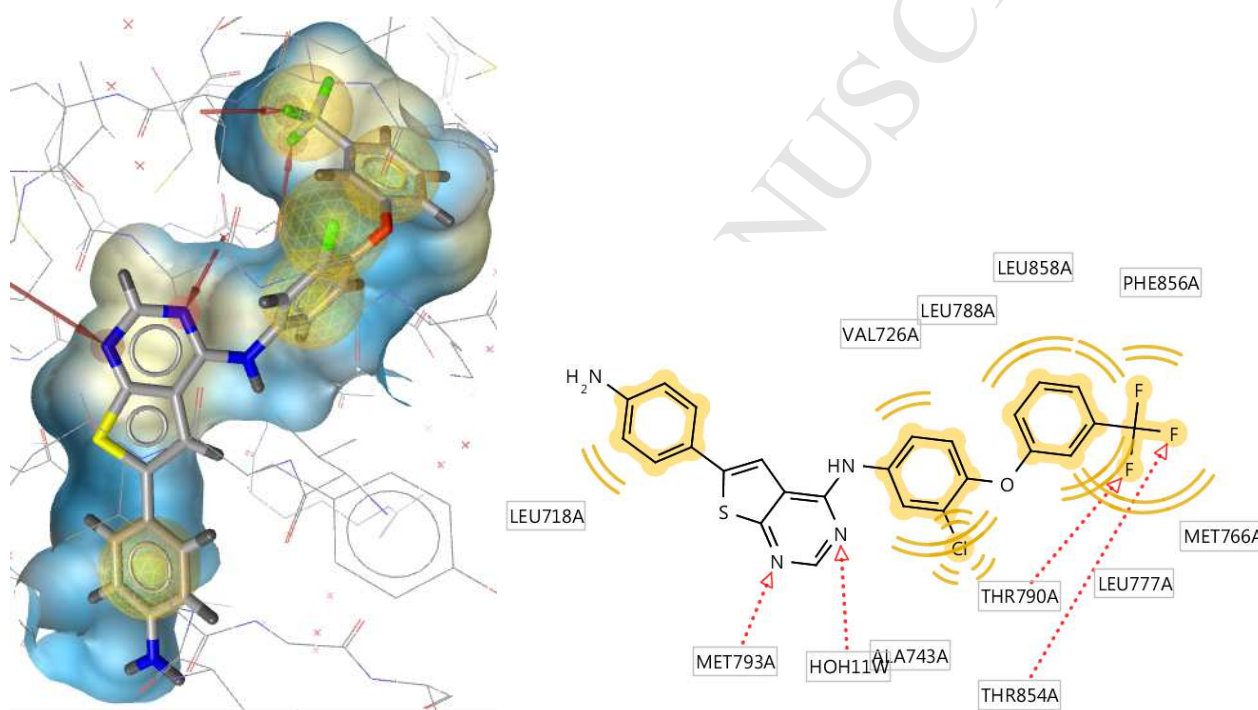
Figure 10 Docking pose of compound **21** in EGFR (PDB: 3POZ) along with its 2D interaction diagram illustrating the interacting amino acids. Interactions are illustrated as follows; red arrow= hydrogen bond acceptor, yellow spheres= hydrophobic interactions. The diagrams were generated using LigandScout 4.2.
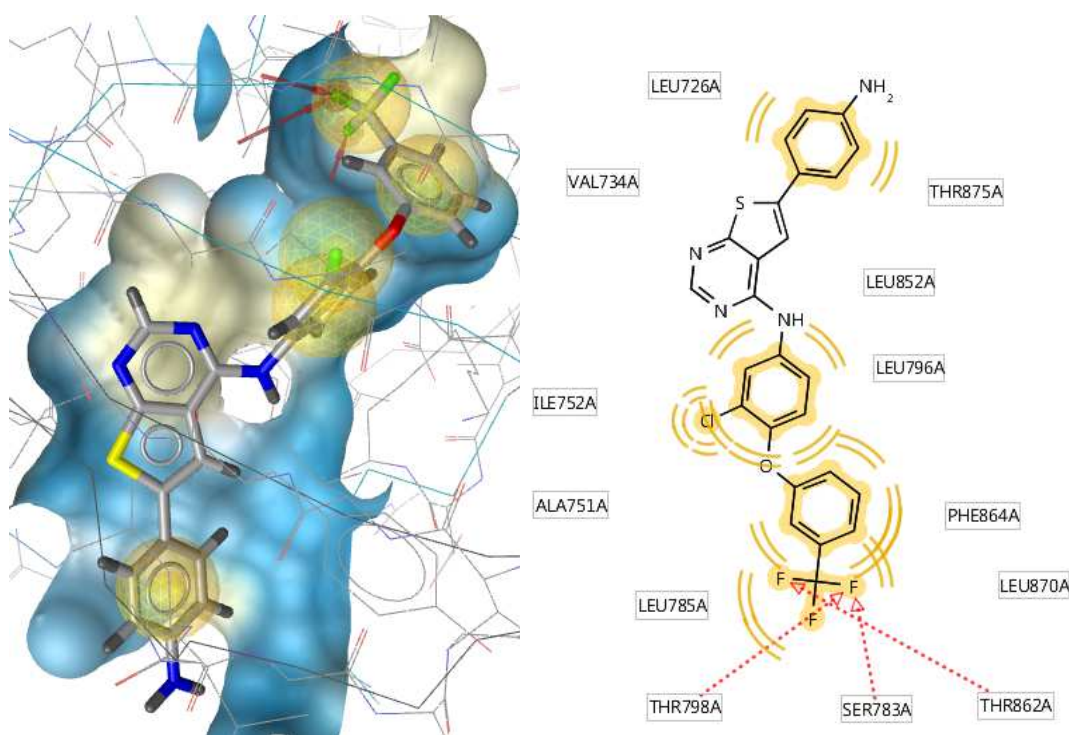
Figure 11 Docking pose of compound **21** in HER2 (PDB: 3RCD) along with its 2D interaction diagram illustrating the interacting amino acids. Interactions are illustrated as follows; red arrow= hydrogen bond acceptor, yellow spheres= hydrophobic interactions. The diagrams were generated using LigandScout 4.2.

3.4.2. Molecular properties affecting the cellular activity

The cellular activity of an enzymatically active compound is affected by other factors governing the cellular permeability of the compound. The balance between the hydrophobicity/hydrophilicity of the compound is one of the main factors affecting its cellular permeability. The hydrophobicity/ hydrophilicity of a compound can be described in terms of different molecular properties like, for instance, the LogP. In order to identify the molecular properties affecting the cellular activity of our target compounds, the correlation between the cellular activity (Log(A431_IC$_{50}$)) and different molecular properties was calculated and a correlation matrix was generated using Accelrys Discovery Studio 2.5 (**Supplementary Figure S5**). The correlation matrix shows that the molecular properties of highest correlation with the cellular activity are the LogP and the Polar Surface Area (PSA), where both properties directly reflect the degree of hydrophobicity/hydrophilicity of the compounds, assuring the influence of the hydrophobicity on the cellular permeability and hence the cellular activity. The two properties (**Supplementary Table S3**) were plotted against Log cellular activity. The plots show a positive correlation between the cellular activity and the ALogP (**Figure 12**),

and a negative correlation between the cellular activity and the PSA (**Figure 13**), meaning that increasing the ALogP and/or decreasing the PSA of the compounds would increase the cellular activity.
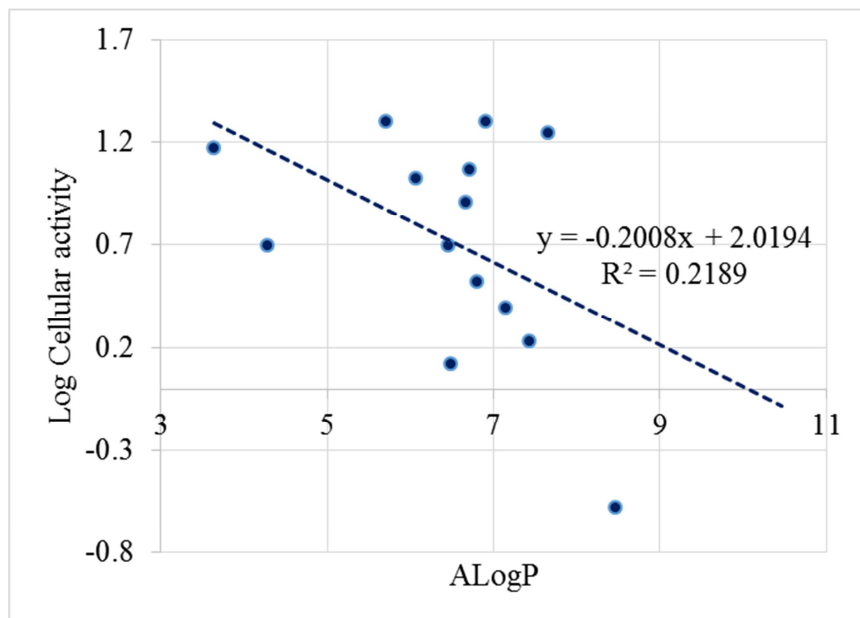
Figure 12 The correlation between the cellular activity and ALogP of the compounds
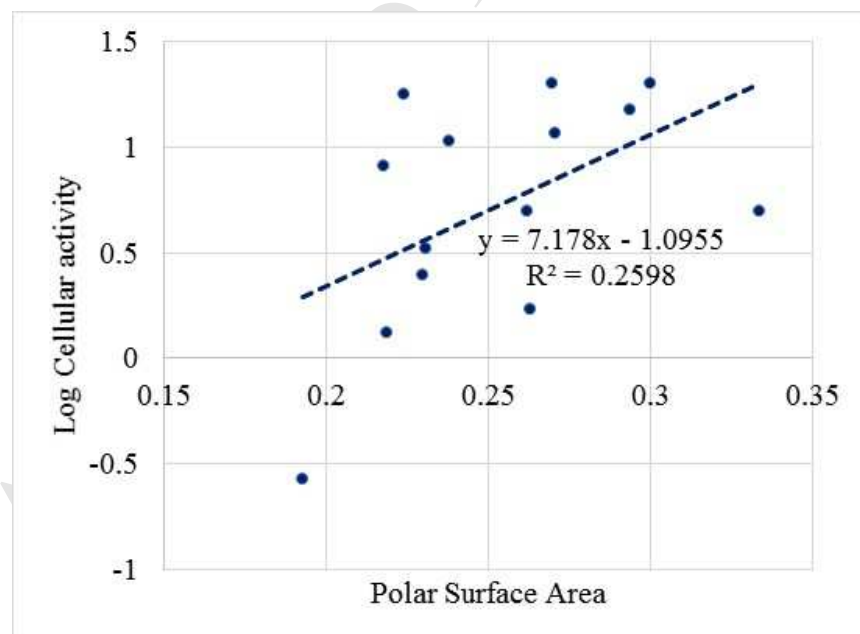
Figure 13 The correlation between the cellular activity and PSA of the compounds

4. Conclusion

We developed a series of thieno[2,3-*d*]pyrimidine-based dual EGFR/HER2 inhibitors with the aim of overcoming the resistance against EGFR inhibitors. Building on the 6-phenylthieno[2,3-*d*]pyrimidine as a core scaffold and a hinge binder, we screened a small targeted library of aniline derivatives in order to identify the aniline headgroup that can attain optimum dual inhibition. Compounds **14a** and **18a**, bearing the bulky aniline headgroups (3-chloro-4-(3-(trifluoromethyl)phenoxy)aniline and 3-chloro-4-((3-fluorobenzyl)oxy)aniline, respectively) that can bind efficiently in the back pocket (as proposed through the docking study), showed the best dual inhibitory activities both enzymatically (with % inhibition at 10 μM against EGFR of 80% and 86%, respectively, and against HER2 of 67% and 72%, respectively) and cellularly (IC$_{50}$ against A431 of 1.72 μM and 11 μM, respectively, and against MDA-MB-361 of 3.65 μM and 7.5 μM, respectively). The impact of increasing the hydrophilicity of the solubilizing group on the dual inhibitory activities of the compounds was demonstrated through the improved activity of the aniline analogue **21** (97% and 96% inhibition against EGFR and HER2 at 10 μM, respectively) compared to its NO$_2$ parent **14a**, however, its cellular antiproliferative activity was hampered by the increased hydrophilicity (IC$_{50}$ of 11.37 μM and 5.85 μM against A431 and MDA-MB-361, respectively) with respect to its NO$_2$ parent. Therefore, a small library of diverse solubilizing groups was screened in order to optimize the enzymatic and cellular activities of **21**. Throughout a series of enzymatic and cell-based assays, **27b** maintained potent dual EGFR/HER2 inhibitory activity with consistently robust anticancer cellular activities. By virtue of its solubilizing group (1-(2-morpholinoethyl)urea), **27b** provided the desirable balance between the degree of hydrophilicity of the solubilizing group required for optimum dual enzymatic activity, and the overall extent of polarity of the compound needed to attain optimum cellular activities. **27b** showed potent dual EGFR/HER2 inhibition with IC$_{50}$ of 91.7 nM and 1.2 μM, respectively. Additionally, **27b** induced apoptotic cell death in MDA-MB-361 cells with IC$_{50}$ of 3.5 μM and an IC$_{50}$ of 1.45 μM against A431, exhibiting superior anti-proliferative activities compared to lapatinib against these cell lines. Moreover, **27b** potently inhibited the EGF-induced activation of EGFR as well as its downstream signaling effectors (AKT/S6K/S6) in A431 cells in a concentration-dependent manner. Finally, in accordance with our proposed design to tackle the T790M mutation, **27b** dramatically impeded the proliferation of NCI-H1975 cell line, harboring the T790M mutation, with IC$_{50}$ of 4.2 μM. Evidently, **27b** inhibited the EGFR T790M signaling pathway in NCI-H1975 cells as illustrated by western blot analysis. On these grounds, **27b** represents a promising candidate for further development of dual EGFR/HER2 inhibitors that can overcome the resistance against currently used EGFR inhibitors.

5. Experimental

5.1. Chemistry

Chemicals were purchased from Sigma-Aldrich (Germany), Merck (Darmstadt, Germany), Alfa Aesar (Germany) and Loba Chemie (India), and were used as such without further purification. Solvents used for column chromatography were redistilled prior to use on BUCHI Rotavapor. Flash column chromatography was performed using silica gel (230-400 mesh particle size) purchased from Sigma-Aldrich. Reactions were followed using analytical thin layer chromatography (TLC), performed on Aluminum silica gel 60 F_{254} TLC plates, purchased from Merck, with visualization under UV light (254 nm). Melting points were recorded on Stuart Scientific apparatus and are reported herein uncorrected. ^{1}HNMR spectra and ^{13}CNMR spectra were determined in δ scale (ppm) and J (Hz) on a Bruker 400 MHz spectrophotometer and referred to TMS at Center for Drug Discovery Research and Development, Ain Shams University. Electrospray-impact ionization mass (EI-MS) spectra were obtained using Thermo Scientific ISQ LT mass spectrometer at the Regional Center for Mycology and Biotechnology, Al-Azhar University. Elemental analyses were carried out on a Thermo Scientific Flash 2000 elemental analyzer at the Regional Center for Mycology and Biotechnology, Al-Azhar University. Intermediates (**2a-d** [32,33], **4a,b** [34,35], **6** [36]) were prepared following similar previously reported procedures (see **supplementary**).

5.1.1. 2-((2-Chloro-4-nitrophenyl)thio)benzo[d]thiazole (7)
A mixture of 2-chloro-1-fluoro-4-nitrobenzene (1 equiv., 2.85 mmol, 0.5 g), benzo[*d*]thiazole-2-thiol (1 equiv., 2.85 mmol, 0.47 g) and anhydrous K_2CO_3 (1.1 equiv., 3.13 mmol, 0.43 g) in dry DMF (10 mL) was heated at 80 °C for 24 hours. After cooling, the reaction mixture was poured into ice/water (100 mL). The precipitated solid was filtered, washed with water, and then washed with cold n-hexane to afford the designated compound (**7**) as pale yellow powder (0.53 g, 58%); MP 104-106 °C.

5.1.2. 4-(Benzo[d]thiazol-2-ylthio)-3-chloroaniline (8)
A mixture of compound (**7**) (1 equiv., 1.54 mmol, 0.5 g) and Stannous chloride dihydrate (5 equiv., 7.74 mmol, 1.74 g) in EtOAc (25 mL) was heated at reflux temperature (80 °C) for 24 hours. After cooling, ice-cold water was added to the reaction mixture and moved to a separating funnel, where the organic layer was washed multiple times with aqueous NaOH (10%), then washed with brine. The organic layer was dried over anhydrous Na_2SO_4 and evaporated under vacuum giving the designated compound (**8**) as buff powder (0.32 g, 71%); MP 128-130 °C.

5.1.3. (E)-N,N-Dimethyl-2-(4-nitrophenyl)ethenamine (9)
A mixture of 4-Nitrotoluene (1 equiv., 0.036 mol, 5 g) and *N,N*-Dimethylformamide dimethyl acetal (2 equiv., 0.072 mol, 8.57 g) in dry DMF (15 mL) was heated at 110 °C

under N_2 for 48 hours. After cooling, the reaction mixture was poured into ice/water (150 mL). The precipitated solid was filtered, washed with water and recrystallized from acetone/H_2O to afford the enamine (**9**) as red crystals (4.83 g, 70%); MP 146-148 ^{o}C; **^{1}H NMR (400 MHz, DMSO-d$_6$)** δ 7.95 (d, J = 9.0 Hz, 2H, ArH), 7.50 (d, J = 13.5 Hz, 1H, -CH=CH-N), 7.27 (d, J = 9.0 Hz, 2H, ArH), 5.19 (d, J = 13.5 Hz, 1H, -CH=CH-N), 2.92 (s, 6H, CH$_3$); **^{13}C NMR (101 MHz, DMSO-d$_6$)** δ 149.49, 146.21, 141.32, 124.79, 122.48, 94.89.

5.1.4.   Ethyl 2-amino-5-(4-nitrophenyl)thiophene-3-carboxylate (**10**)

A mixture of the enamine (**9**) (1 equiv., 0.037 mol, 7.15 g), ethyl cyanoacetate (1 equiv., 0.037 mol, 4.2 g) and elemental sulfur (1 equiv., 0.037 mol, 1.2 g) in absolute ethanol (75 mL) was treated with morpholine (7.5 mL) and heated at reflux temperature (80 ^{o}C) for 24 hours. After cooling, the reaction mixture was poured into ice/water (250 mL). The precipitated solid was filtered over a Celite pad, and then the total solid mass was extracted by EtOAc. The organic layer was dried over anhydrous Na_2SO_4 and evaporated under vacuum giving the designated thiophene derivative (**10**) as brick red powder (9.2 g, 85%); MP 164-165 ^{o}C; **^{1}H NMR (400 MHz, DMSO-d$_6$)** δ 8.15 (d, J = 8.9 Hz, 2H, ArH), 7.81 (s, 2H, NH$_2$), 7.69 (d, J = 8.8 Hz, 2H, ArH), 7.60 (s, 1H, thiophene), 4.24 (q, J = 7.1 Hz, 2H, -CH$_2$-), 1.30 (t, J = 7.1 Hz, 3H, -CH$_3$); **^{13}C NMR (101 MHz, DMSO-d$_6$)** δ 165.68, 164.54, 145.00, 140.94, 126.43, 124.87, 124.57, 119.90, 106.45, 59.85, 14.92.

5.1.5.   6-(4-Nitrophenyl)thieno[2,3-d]pyrimidin-4(3H)-one (**11**)

The thiophene derivative (**10**) (1 equiv., 8.55 mmol, 2.5 g) was suspended in formamide (25 mL) and heated at 200 ^{o}C for 5 hours. After cooling, the reaction mixture was poured into ice/water (250 mL). The precipitated solid was filtered, washed with water, and then washed with petroleum ether to afford the designated thieno[2,3-*d*]pyrimidine derivative (**11**) as golden brown powder (2.1 g, 90%); MP > 300 ^{o}C; **^{1}H NMR (400 MHz, DMSO-d$_6$)** δ 12.64 (s, 1H, NH), 8.23 (d, J = 8.8 Hz, 2H, ArH), 8.17 (s, 1H, pyrimidinone), 8.08 (s, 1H, thiophene), 8.03 (d, J = 8.8 Hz, 2H, ArH); **^{13}C NMR (101 MHz, DMSO-d$_6$)** δ 164.92, 157.15, 146.96, 146.74, 139.03, 136.66, 126.66, 126.27, 124.44, 120.99.

5.1.6.   4-Chloro-6-(4-nitrophenyl)thieno[2,3-d]pyrimidine (**12**)

The thieno[2,3-*d*]pyrimidine (**11**) (1 equiv., 11 mmol, 3 g) was cooled in an ice bath, then phosphorous oxychloride (18 equiv., 198 mmol, 18.5 mL) was added dropwise, then the mixture was heated at reflux temperature (110 ^{o}C) for 24 hours. After cooling, the reaction mixture was slowly poured into ice/water (250 mL), then neutralized with ammonia solution (33%). The precipitated solid was filtered, washed with water, and then extracted with EtOAc. The organic layer was dried over anhydrous Na_2SO_4 and evaporated under vacuum giving the designated compound (**12**) as orange powder (1.6 g, 50%); MP 216-218 ^{o}C; **^{1}H NMR (400 MHz, DMSO-d$_6$)** δ 8.99 (s, 1H, pyrimidine H), 8.35 (d, J = 8.9 Hz, 2H, ArH), 8.32 (s, 1H, thiophene), 8.24 (d, J = 8.9 Hz, 2H, ArH); **^{13}C**

NMR (101 MHz, DMSO-d$_6$) δ 154.08, 148.27, 142.86, 138.42, 132.39, 131.11, 128.45, 125.00, 124.96, 119.04.

5.1.7.   General procedure for the preparation of compounds (13a-d)

To a solution of the 4-chlorothieno[2,3-*d*]pyrimidine derivative (**12**) (1 equiv., 0.34 mmol, 0.1 g) in i-propanol, the respective aniline derivative (*viz*; 3-bromoaniline, 4-chloro-3-(trifluoromethyl)aniline, 3-ethynylaniline, 3-chloro-4-fluoroaniline) (1.2 equiv., 0.4 mmol) was added. The mixture was heated at reflux temperature (85 ^{o}C) for 24-72 hours. After cooling, the reaction mixture was concentrated under vacuum into a residue that was purified by flash column chromatography eluting with CH$_2$Cl$_2$/MeOH (99:1) yielding the designated compounds (**13a-d**).

5.1.7.1.   N-(3-Bromophenyl)-6-(4-nitrophenyl)thieno[2,3-d]pyrimidin-4-amine (13a)

The designated compound was obtained as golden yellow crystals (0.06 g, 41%); MP 279-281 ^{o}C; **^{1}H NMR (400 MHz, DMSO-d$_6$)** δ 9.89 (s, 1H, NH), 8.60 (s, 1H, pyrimidine H), 8.51 (s, 1H, thiophene), 8.39 (d, *J* = 7.3 Hz, 2H, ArH), 8.23 (s, 1H, ArH aniline), 7.97 (d, *J* = 8.7 Hz, 2H, ArH), 7.85 (d, *J* = 8.2 Hz, 1H, ArH aniline), 7.38 (t, *J* = 8.0 Hz, 1H, ArH aniline), 7.30 (d, *J* = 8.0 Hz, 1H, ArH aniline); **^{13}C NMR (101 MHz, DMSO-d$_6$)** δ 167.49, 154.97, 154.52, 147.41, 141.23, 139.60, 137.08, 131.09, 127.08, 126.32, 125.24, 123.65, 121.89, 120.14, 119.20, 118.93; **MS** : (Mwt.: 427.27) : *m/z*, 429 [M$^+$+2, (5.39%)], 427 [M$^+$, (73.93%)], 426 (100%); **Anal**. Calcd for C$_{18}$H$_{11}$BrN$_4$O$_2$S: C, 50.60; H, 2.59; Br, 18.70; N, 13.11; O, 7.49; S, 7.50; Found: C, 50.48; H, 2.71; N, 13.45; S, 7.66.

5.1.7.2.   N-(4-Chloro-3-(trifluoromethyl)phenyl)-6-(4-nitrophenyl)thieno[2,3-d]pyrimidin-4-amine (13b)

The designated compound was obtained as bright yellow crystals (0.03 g, 20%); **^{1}H NMR (400 MHz, DMSO-d$_6$)** δ 10.15 (s, 1H, NH), 8.65 (s, 1H, pyrimidine H), 8.50 (s, 1H, thiophene), 8.44 (d, *J* = 2.5 Hz, 1H, ArH aniline), 8.40 (d, *J* = 8.8 Hz, 2H, ArH), 8.29 (dd, *J* = 8.8, 2.3 Hz, 1H, ArH aniline), 8.00 (d, *J* = 8.8 Hz, 2H, ArH), 7.77 (d, *J* = 8.8 Hz, 1H, ArH aniline); **MS** : (Mwt.: 450.82) : *m/z*, 452.8 [M$^+$+2, (8.99%)], 450.9 [M$^+$, (51%)], 449.9 (100%); **Anal**. Calcd for C$_{19}$H$_{10}$ClF$_3$N$_4$O$_2$S: C, 50.62; H, 2.24; Cl, 7.86; F, 12.64; N, 12.43; O, 7.10; S, 7.11.

5.1.7.3.   N-(3-Ethynylphenyl)-6-(4-nitrophenyl)thieno[2,3-d]pyrimidin-4-amine (13c)

The designated compound was obtained as bright orange crystals (0.08 g, 63%); MP 258-260 ^{o}C; **^{1}H NMR (400 MHz, DMSO-d$_6$)** δ 9.82 (s, 1H, NH), 8.56 (s, 1H, pyrimidine H), 8.48 (s, 1H, thiophene), 8.36 (d, *J* = 8.9 Hz, 2H, ArH), 8.07 (s, 1H, ArH aniline), 7.94 (d, *J* = 8.9 Hz, 2H, ArH), 7.87 (dd, *J* = 8.3, 1.3 Hz, 1H, ArH aniline), 7.42 (t, *J* = 7.9 Hz, 1H, ArH aniline), 7.23 (d, *J* = 7.7 Hz, 1H, ArH aniline), 4.22 (s, 1H, -C≡<u>CH</u>); **MS** : (Mwt.:

372.40) : m/z, 372.8 [M$^+$, (19.85%)], 370.9 (100%); **Anal**. Calcd for C$_{20}$H$_{12}$N$_4$O$_2$S: C, 64.50; H, 3.25; N, 15.04; O, 8.59; S, 8.61; Found: C, 64.82; H, 3.49; N, 15.37; S, 8.49.

5.1.7.4. N-(3-Chloro-4-fluorophenyl)-6-(4-nitrophenyl)thieno[2,3-d]pyrimidin-4-amine (13d)

The designated compound was obtained as bright orange crystals (0.11 g, 80%); MP 315-316 ^{o}C; ^{1}**H NMR (400 MHz, DMSO-d$_6$)** δ 10.19 (s, 1H, NH), 8.70 (s, 1H, pyrimidine H), 8.56 (s, 1H, thiophene), 8.35 (d, J = 8.8 Hz, 2H, ArH), 8.26 (dd, J = 6.8, 2.6 Hz, 1H, ArH aniline), 7.96 (d, J = 8.8 Hz, 2H, ArH), 7.89 – 7.81 (m, 1H, ArH aniline), 7.44 (t, J = 9.1 Hz, 1H, ArH aniline); **MS** : (Mwt.: 400.81) : m/z, 402.9 [M$^+$+2, (7%)], 400.9 [M$^+$, (44.46%)], 398.9 (100%); **Anal**. Calcd for C$_{18}$H$_{10}$ClFN$_4$O$_2$S: C, 53.94; H, 2.51; Cl, 8.85; F, 4.74; N, 13.98; O, 7.98; S, 8.00; Found: C, 54.23; H, 2.72; N, 14.29; S, 7.68.

5.1.8. General procedure for the preparation of compounds (14a,b)

To a solution of the 4-chlorothieno[2,3-d]pyrimidine derivative (**12**) (1 equiv., 0.34 mmol, 0.1 g) in n-butanol, the respective phenoxy aniline derivative (**4a,b**) (1.2 equiv., 0.4 mmol) was added. The mixture was heated at reflux temperature (120 ^{o}C) for 24 hours. After cooling, the reaction mixture was concentrated under vacuum into a residue that was purified by flash column chromatography eluting with CH$_2$Cl$_2$/MeOH (99:1) yielding the designated compounds (**14a,b**).

5.1.8.1. N-(3-Chloro-4-(3-(trifluoromethyl)phenoxy)phenyl)-6-(4-nitrophenyl)thieno[2,3-d]pyrimidin-4-amine (14a)

The designated compound was obtained as bright orange crystals (0.06 g, 32%); MP 220-222 ^{o}C; ^{1}**H NMR (400 MHz, DMSO-d$_6$)** δ 9.99 (s, 1H, NH), 8.62 (s, 1H, pyrimidine), 8.49 (s, 1H, thiophene), 8.39 (d, J = 8.8 Hz, 2H, ArH), 8.31 (d, J = 2.5 Hz, 1H, ArH aniline), 7.98 (d, J = 8.8 Hz, 2H, ArH), 7.87 (dd, J = 8.9, 2.6 Hz, 1H, ArH aniline), 7.63 (t, J = 8.0 Hz, 1H, ArH phenoxy), 7.49 (d, J = 7.8 Hz, 1H, ArH phenoxy), 7.37 (d, J = 8.9 Hz, 1H, ArH aniline), 7.27 (s, 1H, ArH phenoxy), 7.24 (dd, J = 8.2, 2.2 Hz, 1H, ArH phenoxy); **MS** : (Mwt.: 542.92) : m/z, 544 [M$^+$+2, (60%)], 542 [M$^+$, (100%)]; **Anal**. Calcd for C$_{25}$H$_{14}$ClF$_3$N$_4$O$_3$S: C, 55.31; H, 2.60; Cl, 6.53; F, 10.50; N, 10.32; O, 8.84; S, 5.91; Found: C, 55.49; H, 2.45; N, 10.6; S, 6.04.

5.1.8.2. N-(3-Chloro-4-(m-tolyloxy)phenyl)-6-(4-nitrophenyl)thieno[2,3-d]pyrimidin-4-amine (14b)

The designated compound was obtained as brownish orange crystals (0.09 g, 54%); MP 162-164 ^{o}C; ^{1}**H NMR (400 MHz, DMSO-d$_6$)** δ 10.19 (s, 1H, NH), 8.73 (s, 1H, pyrimidine), 8.55 (s, 1H, thiophene), 8.33 (d, J = 8.8 Hz, 2H, ArH), 8.28 (d, J = 2.5 Hz, 1H, ArH aniline), 7.94 (d, J = 8.7 Hz, 2H, ArH), 7.86 (dd, J = 8.6, 2.1 Hz, 1H, ArH aniline), 7.23 (t, J = 7.9 Hz, 1H, ArH phenoxy), 7.16 (d, J = 8.9 Hz, 1H, ArH aniline), 6.91 (d, J = 7.5 Hz, 1H, ArH phenoxy), 6.75 (s, 1H, ArH phenoxy), 6.70 (dd, J = 8.1, 2.5 Hz, 1H, ArH phenoxy), 2.27 (s, 3H, -CH$_3$); **MS** : (Mwt.: 488.95) : m/z, 488 [M$^+$,

(6.79%)], 398 (100%); **Anal**. Calcd for $C_{25}H_{17}ClN_4O_3S$: C, 61.41; H, 3.50; Cl, 7.25; N, 11.46; O, 9.82; S, 6.56; Found: C, 61.28; H, 3.68; N, 11.64; S, 6.7.

5.1.9. N-(1-Benzyl-1H-indazol-5-yl)-6-(4-nitrophenyl)thieno[2,3-d]pyrimidin-4-amine (15)

To a solution of the 4-chlorothieno[2,3-*d*]pyrimidine derivative (**12**) (1 equiv., 0.34 mmol, 0.1 g) in i-propanol, the indazol-5-amine derivative (**6**) (1.2 equiv., 0.4 mmol, 0.09 g) was added. The mixture was heated at reflux temperature (85 °C) for 48 hours. After cooling, the reaction mixture was concentrated under vacuum into a residue that was purified by flash column chromatography eluting with CH_2Cl_2/MeOH/TEA (99:1:0.1) yielding the designated compound (**15**) as brick red crystals (0.065 g, 40%); MP 259-262 °C; **^{1}H NMR (400 MHz, DMSO-d$_6$)** δ 9.89 (s, 1H, NH), 8.51 (s, 1H, pyrimidine), 8.48 (s, 1H, thiophene), 8.37 (d, *J* = 8.9 Hz, 2H, ArH), 8.25 (d, *J* = 1.5 Hz, 1H, ArH indazole), 8.12 (d, *J* = 0.7 Hz, 1H, ArH indazole), 7.96 (d, *J* = 8.9 Hz, 2H, ArH), 7.72 (d, *J* = 8.9 Hz, 1H, ArH indazole), 7.64 (dd, *J* = 9.0, 1.9 Hz, 1H, ArH indazole), 7.33 – 7.20 (m, 5H, ArH benzyl), 5.65 (s, 2H, -CH$_2$- benzyl); **^{13}C NMR (101 MHz, DMSO-d$_6$)** δ 167.23, 155.65, 154.85, 147.28, 139.78, 138.05, 137.17, 136.46, 133.54, 132.47, 129.02, 127.99, 127.80, 126.95, 125.24, 124.25, 123.32, 119.41, 118.56, 113.48, 110.33, 52.43; **MS** : (Mwt.: 478.53) : *m/z*, 478 [M$^+$, (100%)]; **Anal**. Calcd for $C_{26}H_{18}N_6O_2S$: C, 65.26; H, 3.79; N, 17.56; O, 6.69; S, 6.70; Found: C, 65.42; H, 3.87; N, 17.89; S, 6.58.

5.1.10. N-(4-(Benzo[d]thiazol-2-ylthio)-3-chlorophenyl)-6-(4-nitrophenyl)thieno[2,3-d]pyrimidin-4-amine (16)

To a solution of the 4-chlorothieno[2,3-*d*]pyrimidine derivative (**12**) (1 equiv., 0.34 mmol, 0.1 g) in i-propanol, the benzo[*d*]thiazole derivative (**8**) (1.2 equiv., 0.4 mmol, 0.12 g) was added. The mixture was heated at reflux temperature (85 °C) for 72 hours. After cooling, the reaction mixture was concentrated under vacuum into a residue that was purified by flash column chromatography eluting with CH_2Cl_2/MeOH (99:1) yielding the designated compound (**16**) as reddish brown crystals (0.08 g, 43%); MP 286-288 °C; **^{1}H NMR (400 MHz, DMSO-d$_6$)** δ 10.21 (s, 1H, NH), 8.72 (s, 1H, pyrimidine), 8.56 (s, 1H, thiophene), 8.51 (d, *J* = 2.2 Hz, 1H, ArH aniline), 8.42 (d, *J* = 8.9 Hz, 2H, ArH), 8.08 – 8.03 (m, 2H, ArH aniline), 8.02 (d, *J* = 7.4 Hz, 2H, ArH), 7.96 (d, *J* = 7.5 Hz, 1H, ArH benzothiazole), 7.87 (d, *J* = 8.1 Hz, 1H, ArH benzothiazole), 7.47 (td, 1H, ArH benzothiazole), 7.36 (td, 1H, ArH benzothiazole); **^{13}C NMR (101 MHz, DMSO-d$_6$)** δ 167.74, 154.60, 154.28, 153.98, 147.44, 143.92, 139.41, 139.08, 137.60, 135.36, 127.12, 126.98, 126.96, 125.22, 125.00, 122.30, 122.00, 121.91, 120.59, 120.51, 119.29, 118.93; **MS** : (Mwt.: 548.06) : *m/z*, 550 [M$^+$+2, (1.68%)], 548 [M$^+$, (4%)], 512 (100%); **Anal**. Calcd for $C_{25}H_{14}ClN_5O_2S_3$: C, 54.79; H, 2.57; Cl, 6.47; N, 12.78; O, 5.84; S, 17.55; Found: C, 54.47; H, 2.68; N, 13.04; S, 17.82.

5.1.11. General procedure for the preparation of compounds (17a,b)

To a solution of the 4-chlorothieno[2,3-*d*]pyrimidine derivative (**12**) (1 equiv., 0.34 mmol, 0.1 g) in i-propanol, the respective amine (*viz*; benzylamine, phenethylamine) (1.2 equiv., 0.4 mmol) was added. The mixture was heated at reflux temperature (85 °C) for 24-48 hours. After cooling, the reaction mixture was concentrated under vacuum into a residue that was purified by flash column chromatography eluting with CH$_2$Cl$_2$/MeOH (99:1) yielding the designated compounds (**17a,b**).

5.1.11.1. N-Benzyl-6-(4-nitrophenyl)thieno[2,3-d]pyrimidin-4-amine (17a)

The designated compound was obtained as bright yellow crystals (0.1 g, 80%); MP 221-222 °C; **^{1}H NMR (400 MHz, DMSO-d$_6$)** δ 8.64 (t, *J* = 5.8 Hz, 1H, NH), 8.36 (s, 1H, pyrimidine H), 8.32 (d, *J* = 6.5 Hz, 2H, ArH), 8.30 (s, 1H, thiophene), 7.87 (d, *J* = 8.7 Hz, 2H, ArH), 7.37 (d, *J* = 7.0 Hz, 2H, ArH benzyl), 7.32 (t, *J* = 7.5 Hz, 2H, ArH benzyl), 7.24 (t, *J* = 7.1 Hz, 1H, ArH benzyl), 4.75 (d, *J* = 5.8 Hz, 2H, CH$_2$ benzyl); **^{13}C NMR (101 MHz, DMSO-d$_6$)** δ 157.40, 155.31, 153.05, 147.16, 139.91, 139.51, 135.78, 128.88, 127.93, 127.48, 126.81, 125.21, 119.43, 117.97, 43.94; **MS** : (Mwt.: 362.41) : *m/z*, 362 [M$^+$, (90%)], 105.9 (100%); **Anal**. Calcd for C$_{19}$H$_{14}$N$_4$O$_2$S: C, 62.97; H, 3.89; N, 15.46; O, 8.83; S, 8.85; Found: C, 63.3; H, 3.97; N, 15.62; S, 8.93.

5.1.11.2. 6-(4-Nitrophenyl)-N-phenethylthieno[2,3-d]pyrimidin-4-amine (17b)

The designated compound was obtained as yellow crystals (0.067 g, 53%); MP 239-242 °C; **^{1}H NMR (400 MHz, DMSO-d$_6$)** δ 8.42 (s, 1H, NH), 8.37 (d, *J* = 8.9 Hz, 2H, ArH), 8.29 (s, 2H, pyrimidine and thiophene), 7.91 (d, *J* = 8.9 Hz, 2H, ArH), 7.34 – 7.19 (m, 5H, ArH phenethylamine), 3.77 (q, *J* = 14.0, 6.4 Hz, 2H, -NHCH$_2$CH$_2$-), 2.97 (t, 2H, -NHCH$_2$CH$_2$-); **MS** : (Mwt.: 376.43) : *m/z*, 376 [M$^+$, (95.5%)], 284.9 (100%); **Anal**. Calcd for C$_{20}$H$_{16}$N$_4$O$_2$S: C, 63.81; H, 4.28; N, 14.88; O, 8.50; S, 8.52; Found: C, 64.14; H, 4.33; N, 15.12; S, 8.67.

5.1.12. General procedure for the preparation of compounds (18a-d)

To a solution of the 4-chlorothieno[2,3-*d*]pyrimidine derivative (**12**) (1 equiv., 0.34 mmol, 0.1 g) in n-butanol, the respective benzyloxy aniline derivative (**2a-d**) (1.2 equiv., 0.4 mmol) was added. The mixture was heated at reflux temperature (120 °C) for 24-48 hours. After cooling, the reaction mixture was concentrated under vacuum into a residue that was purified by flash column chromatography eluting with CH$_2$Cl$_2$/MeOH (98:2) yielding the designated compounds (**18a-d**).

5.1.12.1. N-(3-Chloro-4-((3-fluorobenzyl)oxy)phenyl)-6-(4-nitrophenyl)thieno[2,3-d]pyrimidin-4-amine (18a)

The designated compound was obtained as chocolate brown crystals (0.04 g, 25%); MP 256-258 °C; **^{1}H NMR (400 MHz, DMSO-d$_6$)** δ 9.84 (s, 1H, NH), 8.55 (s, 1H, pyrimidine H), 8.48 (s, 1H, thiophene), 8.40 (d, *J* = 8.9 Hz, 2H, ArH), 8.06 (d, *J* = 2.6 Hz, 1H, ArH aniline), 7.98 (d, *J* = 8.9 Hz, 2H, ArH), 7.70 (dd, *J* = 8.9, 2.6 Hz, 1H, ArH aniline), 7.51 –

7.45 (m, 1H, ArH benzyloxy), 7.32 (dd, *J* = 16.5, 8.3 Hz, 3H, ArH benzyloxy), 7.19 (td, *J* = 8.8, 2.5 Hz, 1H, ArH aniline), 5.26 (s, 2H, CH$_2$ benzyloxy); **MS** : (Mwt.: 506.94) : *m/z*, 508 [M$^+$+2, (4%)], 506 [M$^+$, (12%)], 397 (100%); **Anal**. Calcd for C$_{25}$H$_{16}$ClFN$_4$O$_3$S: C, 59.23; H, 3.18; Cl, 6.99; F, 3.75; N, 11.05; O, 9.47; S, 6.33; Found: C, 59.5; H, 3.24; N, 11.34; S, 6.29.

5.1.12.2. *N-(3-Chloro-4-((3-chlorobenzyl)oxy)phenyl)-6-(4-nitrophenyl)thieno[2,3-d]pyrimidin-4-amine (**18b**)*

The designated compound was obtained as golden yellow crystals (0.05 g, 28%); MP 262-264 ^{o}C; **^{1}H NMR (400 MHz, DMSO-d$_6$)** δ 9.78 (s, 1H, NH), 8.47 (s, 1H, pyrimidine), 8.42 (s, 1H, thiophene), 8.30 (d, *J* = 7.7 Hz, 2H, ArH), 8.00 (d, *J* = 0.4 Hz, 1H, ArH aniline), 7.88 (d, *J* = 7.6 Hz, 2H, ArH), 7.65 (d, *J* = 8.6 Hz, 1H, ArH aniline), 7.51 (s, 1H, ArH benzyloxy), 7.40 (d, *J* = 9.4 Hz, 3H, ArH benzyloxy), 7.22 (d, *J* = 8.7 Hz, 1H, ArH aniline), 5.19 (s, 2H, CH$_2$ benzyloxy); **^{13}C NMR (101 MHz, DMSO-d$_6$)** δ 161.41, 154.61, 154.22, 154.21, 149.52, 146.87, 142.32, 139.30, 139.22, 136.29, 133.17, 133.10, 130.47, 127.90, 127.89, 127.15, 126.54, 126.01, 124.76, 122.97, 121.13, 114.57, 69.39; **MS** : (Mwt.: 523.39) : *m/z*, 523 [M$^+$, (10.5%)], 511 (100%); **Anal**. Calcd for C$_{25}$H$_{16}$Cl$_2$N$_4$O$_3$S: C, 57.37; H, 3.08; Cl, 13.55; N, 10.70; O, 9.17; S, 6.13; Found: C, 57.61; H, 3.25; N, 10.89; S, 6.01.

5.1.12.3. *N-(3-Chloro-4-((3,4-dichlorobenzyl)oxy)phenyl)-6-(4-nitrophenyl)thieno[2,3-d]pyrimidin-4-amine (**18c**)*

The designated compound was obtained as orange crystals (0.19 g, 41%); MP 260-262 ^{o}C; **^{1}H NMR (400 MHz, DMSO-d$_6$)** δ 9.82 (s, 1H, NH), 8.53 (s, 1H, pyrimidine), 8.45 (s, 1H, thiophene), 8.38 (d, *J* = 8.8 Hz, 2H, ArH), 8.05 (d, *J* = 2.5 Hz, 1H, ArH aniline), 7.95 (d, *J* = 8.7 Hz, 2H, ArH), 7.75 (d, *J* = 1.5 Hz, 1H, ArH benzyloxy), 7.69 (dd, *J* = 8.7, 3.0 Hz, 2H, ArH aniline and benzyloxy), 7.48 (dd, *J* = 8.4, 1.4 Hz, 1H, ArH benzyloxy), 7.27 (d, *J* = 9.1 Hz, 1H, ArH aniline), 5.23 (s, 2H, CH$_2$ benzyloxy); **MS** : (Mwt.: 557.84) : *m/z*, 557.9 [M$^+$, (3.12%)], 512 (100%); **Anal**. Calcd for C$_{25}$H$_{15}$Cl$_3$N$_4$O$_3$S: C, 53.83; H, 2.71; Cl, 19.07; N, 10.04; O, 8.60; S, 5.75; Found: C, 54.07; H, 2.88; N, 10.31; S, 5.89.

5.1.12.4. *N-(3-Chloro-4-(pyridin-2-ylmethoxy)phenyl)-6-(4-nitrophenyl)thieno[2,3-d]pyrimidin-4-amine (**18d**)*

The designated compound was obtained as orange crystals (0.06 g, 36%); MP 256-258 ^{o}C; **^{1}H NMR (400 MHz, DMSO-d$_6$)** δ 9.84 (s, 1H, NH), 8.58 (d, *J* = 4.7 Hz, 1H, ArH pyridinyl), 8.52 (s, 1H, pyrimidine), 8.47 (s, 1H, thiophene), 8.37 (d, *J* = 8.8 Hz, 2H, ArH), 8.05 (d, *J* = 2.6 Hz, 1H, ArH aniline), 7.96 (d, *J* = 8.8 Hz, 2H, ArH), 7.87 (td, *J* = 7.7, 1.7 Hz, 1H, ArH pyridinyl), 7.67 (dd, *J* = 9.0, 2.5 Hz, 1H, ArH aniline), 7.57 (d, *J* = 8.0 Hz, 1H, ArH pyridinyl), 7.35 (t, *J* = 8.0, 4.5 Hz, 1H, ArH pyridinyl), 7.28 (d, *J* = 9.0 Hz, 1H, ArH aniline), 5.27 (s, 2H, -OC̲H̲$_2$-); **^{13}C NMR (101 MHz, DMSO-d$_6$)** δ 156.83, 154.93, 154.57, 154.56, 149.97, 149.55, 147.17, 139.60, 137.58, 136.62, 133.54, 126.82, 125.09, 123.51, 123.27, 121.83, 121.52, 121.42, 119.14, 118.54, 114.73, 71.62; **MS** :

(Mwt.: 489.93) : m/z, 489.8 [M^+, (6.9%)], 397 (100%); **Anal**. Calcd for $C_{24}H_{16}ClN_5O_3S$: C, 58.84; H, 3.29; Cl, 7.24; N, 14.29; O, 9.80; S, 6.54; Found: C, 59.01; H, 3.37; N, 14.58; S, 6.72.

5.1.13. 6-(4-Aminophenyl)-N-benzylthieno[2,3-d]pyrimidin-4-amine (*19*)

A mixture of the nitro derivative (**17a**) (1 equiv., 1 mmol, 0.36 g), reduced iron powder (3 equiv., 3 mmol, 0.16 g) and NH_4Cl (9 equiv., 9 mmol, 0.48 g) in 70% $EtOH/H_2O$ (20 mL) was heated at reflux temperature (70 ^{o}C) for 3 hours. The reaction mixture was filtered over a Celite pad to remove the insoluble iron oxides. The filtrate was evaporated under vacuum to residue, to which EtOAc was added, then the resulting suspension was filtered to remove the inorganic salts. The filtrate was dried over anhydrous Na_2SO_4 and evaporated under vacuum into a residue that was purified by flash column chromatography eluting with CH_2Cl_2/MeOH (98:2) yielding the designated compound (**19**) as brown crystals (0.06 g, 20%); MP 136-138 ^{o}C; **^{1}H NMR (400 MHz, DMSO-d$_6$)** δ 8.25 (s, 1H, NH), 8.21 (s, 1H, pyrimidine), 7.66 (s, 1H, thiophene), 7.26 (dd, J = 15.4, 7.4 Hz, 6H, ArH and benzyl), 7.18 (t, 1H, ArH benzyl), 6.58 (d, J = 7.9 Hz, 2H, ArH), 5.42 (s, 2H, NH_2), 4.67 (d, J = 5.0 Hz, 2H, CH_2 benzyl); **MS** : (Mwt.: 332.42) : m/z, 332 [M^+, (100%)]; **Anal**. Calcd for $C_{19}H_{16}N_4S$: C, 68.65; H, 4.85; N, 16.85; S, 9.65; Found: C, 68.91; H, 4.92; N, 17.23; S, 9.72.

5.1.14. 6-(4-Aminophenyl)-N-(3-chloro-4-((3-fluorobenzyl)oxy)phenyl)thieno[2,3-d]pyrimidin-4-amine (*20*)

A mixture of the nitro derivative (**18a**) (1 equiv., 0.4 mmol, 0.2 g), reduced iron powder (3 equiv., 1.2 mmol, 0.07 g) and NH_4Cl (9 equiv., 3.6 mmol, 0.2 g) in 70% $EtOH/H_2O$ (20 mL) was heated at reflux temperature (70 ^{o}C) for 2 hours. The reaction mixture was filtered over a Celite pad to remove the insoluble iron oxides. The filtrate was evaporated under vacuum to residue, to which EtOAc was added, then the resulting suspension was filtered to remove the inorganic salts. The filtrate was dried over anhydrous Na_2SO_4 and evaporated under vacuum affording crystals of the designated compound (**20**), then the crystals were washed with n-hexane. The designated compound (**20**) was obtained as yellowish green crystals (0.14 g, 100%); MP 236-238 ^{o}C; **^{1}H NMR (400 MHz, DMSO-d$_6$)** δ 9.49 (s, 1H, NH), 8.43 (s, 1H, pyrimidine H), 8.06 (d, J = 2.2 Hz, 1H, ArH aniline), 7.88 (s, 1H, thiophene), 7.71 (dd, J = 8.9, 2.2 Hz, 1H, ArH aniline), 7.47 (dd, J = 14.2, 7.8 Hz, 1H, ArH benzyloxy), 7.40 (d, J = 8.4 Hz, 2H, ArH), 7.32 (t, J = 7.8 Hz, 2H, ArH benzyloxy), 7.26 (d, J = 9.0 Hz, 1H, ArH aniline), 7.18 (t, J = 7.4 Hz, 1H, ArH benzyloxy), 6.67 (d, J = 8.4 Hz, 2H, ArH), 5.57 (s, 2H, NH_2), 5.24 (s, 2H, CH_2 benzyloxy); **MS** : (Mwt.: 476.95) : m/z, 478 [M^++2, (8.33%)], 476 [M^+, (25.2%)], 366.9 (100%); **Anal**. Calcd for $C_{25}H_{18}ClFN_4OS$: C, 62.96; H, 3.80; Cl, 7.43; F, 3.98; N, 11.75; O, 3.35; S, 6.72; Found: C, 63.22; H, 3.89; N, 12.01; S, 6.87.

5.1.15. 6-(4-Aminophenyl)-N-(3-chloro-4-(3-(trifluoromethyl)phenoxy)phenyl)thieno[2,3-d]pyrimidin-4-amine (21)

A mixture of the nitro derivative (**14a**) (1 equiv., 1 mmol, 0.5 g), reduced iron powder (3 equiv., 3 mmol, 0.16 g) and NH$_4$Cl (9 equiv., 9 mmol, 0.48 g) in 70% EtOH/H$_2$O (20 mL) was heated at reflux temperature (70 °C) for 2 hours. The reaction mixture was filtered over a Celite pad to remove the insoluble iron oxides. The filtrate was evaporated under vacuum to residue, to which EtOAc was added, then the resulting suspension was filtered to remove the inorganic salts. The filtrate was dried over anhydrous Na$_2$SO$_4$ and evaporated under vacuum affording crystals of the designated compound (**21**), then the crystals were washed with n-hexane. The designated compound (**21**) was obtained as brownish orange crystals (0.47 g, 100%); MP 210-212 °C; **^{1}H NMR (400 MHz, DMSO-d$_6$)** δ 9.66 (s, 1H, NH), 8.48 (s, 1H, pyrimidine), 8.30 (s, 1H, thiophene), 7.99 – 7.79 (m, 2H, ArH aniline), 7.60 (t, *J* = 7.8 Hz, 1H, ArH phenoxy), 7.45 (d, *J* = 7.5 Hz, 1H, ArH phenoxy), 7.40 (d, *J* = 8.1 Hz, 2H, ArH), 7.32 (d, *J* = 8.9 Hz, 1H, ArH aniline), 7.27 – 7.15 (m, 2H, ArH phenoxy), 6.66 (d, *J* = 8.2 Hz, 2H, ArH), 5.56 (s, 2H, NH$_2$); **^{13}C NMR (101 MHz, DMSO-d$_6$)** δ 165.51, 158.21, 153.68, 152.57, 150.40, 145.33, 142.11, 138.43, 131.87, 127.47, 125.68, 123.27, 122.50, 121.32, 120.68, 120.58, 119.89, 119.84, 119.36, 114.58, 113.29, 113.25, 111.16; **MS** : (Mwt.: 512.93) : *m/z*, 514 [M$^+$+2, (8.4%)], 512 [M$^+$, (92.5%)], 396.9 (100%); **Anal**. Calcd for C$_{25}$H$_{16}$ClF$_3$N$_4$OS: C, 58.54; H, 3.14; Cl, 6.91; F, 11.11; N, 10.92; O, 3.12; S, 6.25; Found: C, 58.67; H, 3.22; N, 11.24; S, 6.17.

5.1.16. N-(4-(4-((3-Chloro-4-(3-(trifluoromethyl)phenoxy)phenyl)amino)thieno[2,3-d]pyrimidin-6-yl)phenyl)acetamide (22)

A solution of the 4-aminophenyl thieno[2,3-*d*]pyrimidine derivative (**21**) (1 equiv., 0.2 mmol, 0.1 g) in THF was cooled in an ice bath, then acetic anhydride (1.2 equiv., 0.24 mmol, 0.025 g) was added dropwise at 0 °C, The reaction mixture was stirred at room temperature for 24 hours. Upon completion of the reaction, the reaction mixture was concentrated under vacuum into a residue that was purified by flash column chromatography eluting with CH$_2$Cl$_2$/MeOH (97:3) yielding the designated compound (**22**) as golden yellow crystals (0.037 g, 35%); MP 252-254 °C; **^{1}H NMR (400 MHz, DMSO-d$_6$)** δ 10.11 (s, 1H, NH amide), 9.76 (s, 1H, NH aniline), 8.48 (s, 1H, pyrimidine), 8.24 (s, 1H, thiophene), 8.07 (s, 1H, ArH aniline), 7.81 (d, *J* = 9.1 Hz, 1H, ArH aniline), 7.67 (d, *J* = 8.3 Hz, 2H, ArH), 7.61 (d, *J* = 8.2 Hz, 2H, ArH), 7.55 (t, *J* = 7.7 Hz, 1H, ArH phenoxy), 7.41 (d, *J* = 7.3 Hz, 1H, ArH phenoxy), 7.28 (d, *J* = 8.8 Hz, 1H, ArH aniline), 7.21 – 7.11 (m, 2H, ArH phenoxy), 2.01 (s, 3H, CH$_3$ amide); **^{13}C NMR (101 MHz, DMSO-d$_6$)** δ 169.03, 166.29, 158.16, 154.24, 153.37, 145.56, 145.54, 140.51, 140.22, 138.19, 131.91, 127.97, 126.88, 125.67, 123.28, 123.26, 122.72, 121.52, 120.65, 119.95, 119.08, 114.34, 113.35, 113.32, 24.55; **MS** : (Mwt.: 554.97) : *m/z*, 554 [M$^+$, (21%)], 398.9 (100%); **Anal**. Calcd for C$_{27}$H$_{18}$ClF$_3$N$_4$O$_2$S: C, 58.43; H, 3.27; Cl, 6.39; F, 10.27; N, 10.10; O, 5.77; S, 5.78; Found: C, 58.75; H, 3.39; N, 9.98; S, 5.91.

5.1.17. N-(4-(4-((3-Chloro-4-(3-(trifluoromethyl)phenoxy)phenyl)amino)thieno[2,3-d]pyrimidin-6-yl)phenyl)methanesulfonamide (23)

A solution of the 4-aminophenyl thieno[2,3-*d*]pyrimidine derivative (**21**) (1 equiv., 0.2 mmol, 0.1 g) in pyridine was cooled in an ice bath, then methanesulfonyl chloride (1.2 equiv., 0.24 mmol, 0.026 g) was added dropwise at 0 °C, The reaction mixture was stirred at room temperature for 24 hours. Upon completion of the reaction, the reaction mixture was poured into acidified ice/water (250 mL), then extracted with EtOAc. The organic layer was dried over anhydrous Na_2SO_4 and concentrated under vacuum into a residue that was purified by flash column chromatography eluting with CH_2Cl_2/MeOH (99:1) yielding the designated compound (**23**) as buff crystals (0.035 g, 35%); MP 266-268 °C; **^{1}H NMR (400 MHz, DMSO-d$_6$)** δ 10.04 (s, 1H, NH sulfonamide), 9.85 (s, 1H, NH aniline), 8.56 (s, 1H, pyrimidine), 8.31 (d, *J* = 2.5 Hz, 1H, ArH aniline), 8.16 (s, 1H, thiophene), 7.87 (dd, *J* = 8.9, 2.5 Hz, 1H, ArH aniline), 7.71 (d, *J* = 8.6 Hz, 2H, ArH), 7.62 (t, *J* = 8.0 Hz, 1H, ArH phenoxy), 7.48 (d, *J* = 7.8 Hz, 1H, ArH phenoxy), 7.35 (dd, *J* = 8.7, 1.8 Hz, 3H, ArH and aniline), 7.28 – 7.17 (m, 2H, ArH phenoxy), 3.07 (s, 3H, CH_3 sulfonamide); **^{13}C NMR (101 MHz, DMSO-d$_6$)** δ 166.39, 158.15, 154.34, 153.52, 143.48, 139.85, 139.65, 138.14, 138.13, 131.94, 128.64, 127.48, 125.66, 123.29, 122.84, 122.56, 121.67, 121.66, 120.70, 120.69, 120.31, 119.04, 114.70, 40.10; **MS** : (Mwt.: 591.02) : *m/z*, 592.9 [M$^+$+2, (4.73%)], 590.9 [M$^+$, (14.9%)], 511 (100%); **Anal**. Calcd for $C_{26}H_{18}ClF_3N_4O_3S_2$: C, 52.84; H, 3.07; Cl, 6.00; F, 9.64; N, 9.48; O, 8.12; S, 10.85; Found: C, 53.07; H, 3.23; N, 9.21; S, 10.93.

5.1.18. Ethyl (4-(4-((3-chloro-4-(3-(trifluoromethyl)phenoxy)phenyl)amino)thieno[2,3-d]pyrimidin-6-yl)phenyl)carbamate (24)

A solution of the 4-aminophenyl thieno[2,3-*d*]pyrimidine derivative (**21**) (1 equiv., 0.2 mmol, 0.1 g) in anhydrous pyridine was cooled in an ice bath and purged with N_2, then ethyl chloroformate (1.2 equiv., 0.24 mmol, 0.025 g) was added dropwise at 0 °C, The reaction mixture was stirred under N_2 atmosphere at room temperature for 24 hours. Upon completion of the reaction, the reaction mixture was poured into acidified ice/water (250 mL), then extracted with EtOAc. The organic layer was dried over anhydrous Na_2SO_4 and concentrated under vacuum into a residue that was purified by flash column chromatography eluting with 50% EtOAc in hexane (v/v) yielding the designated compound (**24**) as bright yellow crystals (0.046 g, 40%); MP 190-192 °C; **^{1}H NMR (400 MHz, DMSO-d$_6$)** δ 9.87 (s, 1H, NH carbamate), 9.84 (s, 1H, NH aniline), 8.54 (s, 1H, pyrimidine), 8.30 (d, *J* = 2.5 Hz, 1H, ArH aniline), 8.12 (s, 1H, thiophene), 7.87 (dd, *J* = 8.9, 2.5 Hz, 1H, ArH aniline), 7.66 (d, *J* = 8.8 Hz, 2H, ArH), 7.60 (dd, *J* = 8.3, 5.0 Hz, 3H, ArH and phenoxy), 7.46 (d, *J* = 7.4 Hz, 1H, ArH phenoxy), 7.33 (d, *J* = 8.9 Hz, 1H, ArH aniline), 7.26 – 7.17 (m, 2H, ArH phenoxy), 4.14 (q, *J* = 7.1 Hz, 2H, -O$\underline{CH_2}$CH$_3$), 1.25 (t, *J* = 7.1 Hz, 3H, -OCH$_2$$\underline{CH_3}$); **^{13}C NMR (101 MHz, DMSO-d$_6$)** δ 166.25, 158.22, 158.16, 154.23, 153.92, 153.34, 145.55, 140.53, 140.29, 138.20, 131.92, 127.36, 126.99,

125.66, 123.28, 122.73, 121.76, 121.57, 121.55, 120.68, 120.65, 119.10, 119.08, 114.16, 60.85, 14.96; **MS** : (Mwt.: 585.00) : *m/z*, 587 [M^++2, (1.89%)], 585 [M^+, (6.4%)], 538 (100%); **Anal**. Calcd for $C_{28}H_{20}ClF_3N_4O_3S$: C, 57.49; H, 3.45; Cl, 6.06; F, 9.74; N, 9.58; O, 8.20; S, 5.48; Found: C, 57.23; H, 3.67; N, 9.89; S, 5.62.

5.1.19. (E)-N-(4-(4-((3-Chloro-4-(3-(trifluoromethyl)phenoxy)phenyl)amino)thieno[2,3-d]pyrimidin-6-yl)phenyl)-4-methylpent-2-enamide (25)

A mixture of the 4-aminophenyl thieno[2,3-*d*]pyrimidine derivative (**21**) (1 equiv., 0.2 mmol, 0.1 g), 4-methyl-pent-2-enoic acid (1 equiv., 0.2 mmol, 0.022 g), EDC.HCl (2 equiv., 0.4 mmol, 0.074 g) and DMAP (2 equiv., 0.4 mmol, 0.047 g) in dry DMF was stirred under N_2 atmosphere at room temperature for 24 hours. Upon completion of the reaction, the reaction mixture was poured into ice/water (250 mL), then extracted with EtOAc. The organic layer was dried over anhydrous Na_2SO_4 and concentrated under vacuum into a residue that was purified by flash column chromatography eluting with 50% EtOAc in hexane (v/v) yielding the designated compound (**25**) as light brown crystals (0.025 g, 10%); **^{1}H NMR (400 MHz, DMSO-d$_6$)** δ 10.14 (d, *J* = 41.2 Hz, 1H, NH amide), 9.81 (s, 1H, NH aniline), 8.52 (s, 1H, pyrimidine), 8.28 (s, 1H, thiophene), 8.12 (s, 1H, ArH aniline), 7.84 (d, *J* = 8.6 Hz, 1H, ArH aniline), 7.78 (d, *J* = 8.4 Hz, 2H, ArH), 7.69 (dd, *J* = 20.3, 8.4 Hz, 2H, ArH), 7.58 (t, *J* = 7.9 Hz, 1H, ArH phenoxy), 7.44 (d, *J* = 7.1 Hz, 1H, ArH phenoxy), 7.31 (d, *J* = 8.8 Hz, 1H, ArH aniline), 7.24 – 7.13 (m, 2H, ArH phenoxy), 6.80 (dd, *J* = 15.3, 6.2 Hz, 1H, -CH-CH=CH-CO), 6.05 (d, *J* = 15.4 Hz, 1H, -CH-CH=CH-CO), 3.05 (d, *J* = 6.6 Hz, 1H, -CH(CH$_3$)$_2$), 1.68 (s, 1H, -CH(CH$_3$)$_2$), 1.62 (s, 1H, -CH(CH$_3$)$_2$), 1.02 (d, *J* = 6.7 Hz, 4H, -CH(CH$_3$)$_2$).

5.1.20. (Z)-4-((4-(4-((3-Chloro-4-(3-(trifluoromethyl)phenoxy)phenyl)amino)thieno[2,3-d]pyrimidin-6-yl)phenyl)amino)-4-oxobut-2-enoic acid (26)

To a stirred solution of the 4-aminophenyl thieno[2,3-*d*]pyrimidine derivative (**21**) (1 equiv., 0.2 mmol, 0.1 g) in THF, maleic anhydride (1.2 equiv., 0.24 mmol, 0.023 g) in THF was added dropwise. The reaction mixture was stirred at room temperature for 24 hours. Upon completion of the reaction, the reaction mixture was concentrated under vacuum into a residue that was triturated with H_2O giving yellow crystals which was further purified by flash column chromatography eluting with CH_2Cl_2/MeOH (80:20) yielding the designated compound (**26**) as greenish yellow crystals (0.07 g, 59%); MP 230-232 ^{o}C; **^{1}H NMR (400 MHz, DMSO-d$_6$)** δ 13.66 (s, 1H, OH acid), 10.13 (s, 1H, NH aniline), 8.51 (s, 1H, pyrimidine), 8.43 (s, 1H, thiophene), 8.37 (d, *J* = 2.3 Hz, 1H, ArH aniline), 7.97 (dd, *J* = 8.9, 2.3 Hz, 1H, ArH aniline), 7.75 (d, *J* = 8.6 Hz, 2H, ArH), 7.68 (d, *J* = 8.5 Hz, 2H, ArH), 7.58 (t, *J* = 8.0 Hz, 1H, ArH phenoxy), 7.43 (d, *J* = 7.5 Hz, 1H, ArH phenoxy), 7.30 (d, *J* = 8.9 Hz, 1H, ArH aniline), 7.22 (s, 1H, ArH phenoxy), 7.18 (d, *J* = 8.2 Hz, 1H, ArH phenoxy), 6.23 (d, *J* = 12.8 Hz, 1H, -CH=CH-), 6.03 (d, *J* = 12.8 Hz, 1H, -CH=CH-); **^{13}C NMR (101 MHz, DMSO-d$_6$)** δ 169.00, 166.27, 164.21, 158.24,

154.34, 153.35, 145.29, 140.55, 139.84, 138.55, 131.91, 131.01, 130.95, 128.22, 126.89, 125.58, 123.21, 122.85, 122.69, 121.61, 120.52, 120.11, 119.82, 119.24, 115.59, 113.24, 113.20; **MS** : (Mwt.: 610.99) : *m/z*, 610 [M$^+$, (3.39%)], 351 (100%); **Anal**. Calcd for C$_{29}$H$_{18}$ClF$_3$N$_4$O$_4$S: C, 57.01; H, 2.97; Cl, 5.80; F, 9.33; N, 9.17; O, 10.47; S, 5.25; Found: C, 57.34; H, 3.06; N, 9.93; S, 5.37.

5.1.21. General procedure for the preparation of compounds (27a,b)

A mixture of the 4-aminophenyl thieno[2,3-*d*]pyrimidine derivative (**21**) (1 equiv., 0.2 mmol, 0.1 g) and triphosgene (1 equiv., 0.2 mmol, 0.058 g) in anhydrous THF was heated at 70 ^{o}C under N$_2$ atmosphere for 4 hours. After cooling, the reaction mixture was concentrated under vacuum into a dry residue of the isocyanate intermediate that was used directly for the next step without further purification.

A mixture of the isocyanate and the respective amine (*viz*; cyclopropylamine, 4-(2-Aminoethyl)morpholine) (2 equiv., 0.4 mmol) in anhydrous THF was heated at 70 ^{o}C under N$_2$ atmosphere for 24 hours. Upon completion of the reaction, the reaction mixture was concentrated under vacuum into a residue that was purified by flash column chromatography eluting with CH$_2$Cl$_2$/MeOH (95:5) yielding the designated compounds (**27a,b**).

5.1.21.1. 1-(4-(4-((3-Chloro-4-(3-(trifluoromethyl)phenoxy)phenyl)amino)thieno[2,3-d]pyrimidin-6-yl)phenyl)-3-cyclopropylurea (27a)

The designated compound was obtained as buff crystals (0.04 g, 35%); MP 298-300 ^{o}C; **^{1}H NMR (400 MHz, DMSO-d$_6$)** δ 9.79 (s, 1H, cyclopropyl-NHCO<u>NH</u>-Aryl), 8.56 (s, 1H, NH aniline), 8.46 (s, 1H, pyrimidine), 8.24 (d, *J* = 1.3 Hz, 1H, ArH aniline), 8.06 (s, 1H, thiophene), 7.81 (d, *J* = 8.3 Hz, 1H, ArH aniline), 7.51 (dd, *J* = 22.1, 8.2 Hz, 5H, ArH and phenoxy), 7.39 (d, *J* = 6.5 Hz, 1H, ArH phenoxy), 7.27 (d, *J* = 8.3 Hz, 1H, ArH aniline), 7.19 – 7.08 (m, 2H, ArH phenoxy), 6.45 (s, 1H, cyclopropyl-<u>NH</u>CONH-Aryl), 1.14 (s, 1H, -<u>CH</u>(CH$_2$)$_2$), 0.56 (d, *J* = 5.7 Hz, 2H, -CH(<u>CH$_2$</u>)$_2$), 0.34 (d, *J* = 1.4 Hz, 2H, -CH(<u>CH$_2$</u>)$_2$); **^{13}C NMR (101 MHz, DMSO-d$_6$)** δ 170.73, 166.78, 158.12, 156.33, 154.17, 152.47, 145.83, 141.91, 140.92, 140.91, 137.92, 131.93, 126.90, 125.91, 125.64, 123.21, 123.12, 121.94, 120.67, 119.93, 119.32, 118.60, 113.37, 113.36, 22.85, 6.85; **Anal**. Calcd for C$_{29}$H$_{21}$ClF$_3$N$_5$O$_2$S: C, 58.44; H, 3.55; Cl, 5.95; F, 9.56; N, 11.75; O, 5.37; S, 5.38; Found: C, 58.67; H, 3.7; N, 11.93; S, 5.47.

5.1.21.2. 1-(4-(4-((3-Chloro-4-(3-(trifluoromethyl)phenoxy)phenyl)amino)thieno[2,3-d]pyrimidin-6-yl)phenyl)-3-(2-morpholinoethyl)urea (27b)

The designated compound was obtained as off-white crystals (0.045 g, 35%); MP 294-296 ^{o}C; **^{1}H NMR (400 MHz, DMSO-d$_6$)** δ 9.76 (s, 1H, alkyl-NHCO<u>NH</u>-aryl), 8.88 (s, 1H, NH aniline), 8.50 (s, 1H, pyrimidine), 8.28 (s, 1H, ArH aniline), 8.06 (s, 1H, thiophene), 7.84 (dd, *J* = 8.9, 1.6 Hz, 1H, ArH aniline), 7.54 (dd, *J* = 21.5, 7.3 Hz, 5H, ArH and phenoxy), 7.44 (d, *J* = 7.6 Hz, 1H, ArH phenoxy), 7.31 (d, *J* = 8.8 Hz, 1H, ArH

aniline), 7.23 – 7.13 (m, 2H, ArH phenoxy), 6.15 (t, J = 4.7 Hz, 1H, alkyl-<u>NH</u>CONH-aryl), 3.56 (s, 4H, O(<u>CH$_2$</u>CH$_2$)$_2$N-), 3.19 (d, J = 5.4 Hz, 4H, O(CH$_2$<u>CH$_2$</u>)$_2$N-), 2.36 (s, 4H, -N<u>CH$_2$CH$_2$</u>NH-); **^{13}C NMR (101 MHz, DMSO-d$_6$)** δ 166.10, 158.17, 155.38, 154.25, 154.13, 153.22, 145.52, 142.00, 140.69, 138.24, 131.93, 131.03, 126.96, 125.96, 125.67, 123.31, 122.70, 121.52, 120.65, 119.96, 119.15, 118.42, 113.55, 107.11, 66.67, 58.26, 53.72, 36.49; **MS** : (Mwt.: 669.12) : m/z, 669 [M$^+$, (0.99%)], 368 (100%); **Anal**. Calcd for C$_{32}$H$_{28}$ClF$_3$N$_6$O$_3$S: C, 57.44; H, 4.22; Cl, 5.30; F, 8.52; N, 12.56; O, 7.17; S, 4.79; Found: C, 57.71; H, 4.08; N, 12.78; S, 4.85.

5.2. Biological evaluation

5.2.1. *In vitro* EGFR/HER2 kinase inhibitory assays

The assays were performed in BPS Bioscience Corporation, San Diego, CA, USA (www.bpsbioscience.com). Kinases used in this study were EGFR (BPS catalog # 40187, Lot # 160511-G2) and HER2 (BPS catalog # 40230, Lot # 141211-B4). The substrate Poly-(Glu, Tyr) (Sigma # P7244) and Kinase-Glo Plus Luminescence kinase assay kit (Promega # V3772) were used in this study (see **supplementary**).

5.2.2. Cell-based assays

5.2.2.1. *Materials*

Lapatinib di-p-toluenesulfonate (Cat No. L-4804) was purchased from LC laboratories (USA). RPMI-1640 medium, DMEM medium and fetal bovine serum were purchased from Lonza (USA). Sulforhodamine B sodium salt (Cat No. S1402) was purchased from Sigma Aldrich (USA). Trichloroacetic acid (TCA) was purchased from VWR Prolab Chemicals, International LLC (USA). The following antibodies were used in this study: Primary antibodies against p-mTOR (S2448) (5536), mTOR (2972), p-p70 S6 kinase (T389) (9234), total S6k, pS6 (S235/236) (2211), total S6 (54D2), pAKT (ser 473) (9271), total AKT (9272), and p-EGFR (Y1068) (3777) were purchased from Cell Signalling Technology. Monoclonal anti-vinculin and anti-β-actin were purchased from Sigma Aldrich. Antibody against Annexin V-APC (Cat. No. BMS306APC-100) was purchased from Invitrogen, Thermoscientific Fischer, eBioscience™. All other chemicals and solvents were of highest grade commercially available.

5.2.2.2. *Human cancer cell lines and cell culture*

Human breast adenocarcinoma (SKBr3 and MDA-MB-361) and epidermoid carcinoma (A431) cells were obtained from American Type Culture Collection (ATCC) and maintained as monolayer cultures in Dulbecco's Modified Eagle's medium (DMEM) supplemented with 2mM L-glutamine, 10% FBS and 1% penicillin-streptomycin. Human non-small lung cancer (NCI-H1975) cells were cultured in Roswell Park Memorial Institute medium (RPMI-1640) supplemented with 2mM L-glutamine, 10% FBS and 1%

penicillin-streptomycin. Cells were maintained in a humidified tissue culture incubator at 37ºC with 5 % CO_2 and subcultured to preconfluency after trypsinization (0.5 % trypsin/2.6 mM EDTA).

5.2.2.3. *Cell viability assay*

Cell proliferation was determined using sulphorhodamine B (SRB) cytotoxicity assay as previously described [49]. Briefly, cells were seeded into 96-well plates and grown for 24h. Cells were then treated with either 0.1% DMSO or varying concentrations (0.3125-20 µM) of the test compounds or lapatinib for 72 h. Cells were treated with either 0.1% DMSO or varying concentrations (0.3125-20 µM) of the synthesized compounds or lapatinib for 72 h. Cells were then fixed with ice cold 50 % TCA for 1 h at 4 ºC and stained with 50 µl 0.4 % SRB (Sigma Aldrich) for 30 min at room temperature. SRB was then solubilized with 10 mM tris base (pH 10.5). The optical density (O.D.) was measured at 560 nm using GloMax® multimicroplate reader (Promega, USA).The survival fraction was calculated as follows: O.D. (treated cells)/ O.D. (vehicle-treated cells) [49]. The IC_{50} was calculated using GraphPad Prism software (San Diego, CA, USA).

5.2.2.4. *Apoptosis detection using Annexin V/PI staining*

Cells positive of apoptosis and necrosis were assessed using Annexin V/propidium iodide assay. Phosphatidyl serine externalization which is used as a marker of early-stage apoptosis was detected by Annexin V antibody conjugated to APC, whereas membrane damage due to late-stage apoptosis/necrosis was detected by the binding of PI to nuclear DNA. Cells were treated as indicated. Cells were then harvested, spin down at 3000 rpm for 5 min and washed in PBS. Cells were then fixed in 70% ethanol on ice. Cells were washed in 1% BSA in PBS, stained with propidium iodide overnight at 4°C and analysed using flowcytometer (FACS Calibur, Beckman Coulter). For each sample, 20 000 cells were analyzed. Live (annexin V^-, PI^-) cells, early apoptotic (annexin V^+, PI^-) and late apoptotic- necrotic (annexin V^+, PI^+ and annexin V^-, PI^+) were expressed as percentages of the 20 000 cells and were analyzed using FlowJo software.

5.2.3. Western blotting

Serum-starved A431 and NCI-H1975 cells were treated with varying concentrations of compounds **21** and **27b** and then stimulated with 50 ng/ml EGF for 10 min. SKBr3 and NCI-H1975 cells were treated with **22** and **27b**, respectively, for 72h. Cell lysis and immunoblotting were carried out as described previously [50]. Briefly, cells were harvested and lysed in HEPES lysis buffer [50]. Protein content of cell lysates was determined using Bio-Rad protein assay and then resolved on 12% SDS-PAGE and transferred to nitrocellulose membrane using a wet transfer system (Biorad). The membrane was blocked with 5% skimmed milk in TBST for 1 h and then incubated with the indicated primary antibodies. The membrane was washed twice with TBST and blotted with horseradish peroxidase-conjugated secondary antibody at room temperature

for 1 h and then washed in TBST twice. Protein bands were detected with a chemiluminescence western blot detection kit (Amersham Pharmacia Biotech, Piscataway, NJ, USA).

5.3. Molecular docking study

Molecular Docking was performed using CDOCKER protocol in Accelrys Discovery Studio® 2.5 (Accelrys Inc., San Diego, CA, USA) at the drug design laboratory, Faculty of Pharmacy, Ain Shams University (see **supplementary**).

Author Contributions

K.A.M. Abouzid designed the whole study. D.S. Lasheen and R.A.T. Serya supervised the chemistry work. S.N. Milik synthesized the compounds, performed the molecular modeling study, discussed results and prepared this manuscript. A.K. Abdel-Aziz designed and performed all cell-based assays (biological evaluation of the compounds), analyzed data and discussed results. S. Minucci supervised the biology work, provided intellectual and technical support and discussed results. All the authors reviewed and approved the manuscript.

6. References

[1] P. Blume-Jensen, T. Hunter, Oncogenic kinase signalling., Nature. 411 (2001) 355–65. doi:10.1038/35077225.

[2] F. Ciardiello, G. Tortora, EGFR Antagonists in Cancer Treatment, N. Engl. J. Med. 358 (2008) 1160–1174. doi:10.1056/NEJMra0707704.

[3] A. Citri, Y. Yarden, EGF-ERBB signalling: towards the systems level., Nat. Rev. Mol. Cell Biol. 7 (2006) 505–16. doi:10.1038/nrm1962.

[4] N.E. Hynes, H. a Lane, ERBB receptors and cancer: the complexity of targeted inhibitors., Nat. Rev. Cancer. 5 (2005) 341–54. doi:10.1038/nrc1609.

[5] E.K. Rowinsky, The erbB Family: Targets for Therapeutic Development Against Cancer and Therapeutic Strategies Using Monoclonal Antibodies and Tyrosine Kinase Inhibitors, Annu. Rev. Med. 55 (2004) 433–457. doi:10.1146/annurev.med.55.091902.104433.

[6] M.A. Lemmon, J. Schlessinger, Cell Signaling by Receptor Tyrosine Kinases, Cell. 141 (2010) 1117–1134. doi:10.1016/j.cell.2010.06.011.

[7] R. Bianco, T. Gelardi, V. Damiano, F. Ciardiello, G. Tortora, Rational bases for the development of EGFR inhibitors for cancer treatment, Int. J. Biochem. Cell Biol. 39 (2007) 1416–1431. doi:10.1016/j.biocel.2007.05.008.

[8] S. Kamath, J.K. Buolamwini, Targeting EGFR and HER-2 receptor tyrosine kinases for cancer drug discovery and development, Med. Res. Rev. 26 (2006) 569–594. doi:10.1002/med.20070.

[9] Cancer Research UK, The 10 Most Common Causes of Cancer Death, World, 2012 Estimates, (2014). http://www.cancerresearchuk.org/health-professional/cancer-statistics/worldwide-cancer/mortality#ref1 (accessed June 1, 2017).

[10] R. Roskoski, USFDA approved protein kinase inhibitors, (n.d.). http://www.brimr.org/PKI/PKIs.htm.

[11] S.N. Milik, D.S. Lasheen, R.A.T. Serya, K.A.M. Abouzid, How to train your inhibitor: Design strategies to overcome resistance to Epidermal Growth Factor Receptor inhibitors, Eur. J. Med. Chem. 142 (2017) 131–151. doi:10.1016/j.ejmech.2017.07.023.

[12] E.L. Stewart, S.Z. Tan, G. Liu, M. Tsao, Known and putative mechanisms of resistance to EGFR targeted therapies in NSCLC patients with EGFR mutations — a review, Transl. Lung Cancer Res. 4 (2015) 67–81. doi:10.3978/j.issn.2218-6751.2014.11.06.

[13] K. Takezawa, V. Pirazzoli, M.E. Arcila, C.A. Nebhan, X. Song, E. de Stanchina, K. Ohashi, Y.Y. Janjigian, P.J. Spitzler, M.A. Melnick, G.J. Riely, M.G. Kris, V.A. Miller, M. Ladanyi, K. Politi, W. Pao, HER2 Amplification: A Potential Mechanism of Acquired Resistance to EGFR Inhibition in EGFR-Mutant Lung

Cancers That Lack the Second-Site EGFRT790M Mutation, Cancer Discov. 2 (2012) 922–933. doi:10.1158/2159-8290.CD-12-0108.

[14] N. Tebbutt, M.W. Pedersen, T.G. Johns, Targeting the ERBB family in cancer: couples therapy, Nat. Rev. Cancer. 13 (2013) 663–673. doi:10.1038/nrc3559.

[15] D. Graus-Porta, R.R. Beerli, J.M. Daly, N.E. Hynes, ErbB-2, the preferred heterodimerization partner of all ErbB receptors, is a mediator of lateral signaling, EMBO J. 16 (1997) 1647–1655. doi:10.1093/emboj/16.7.1647.

[16] A.E.G. Lenferink, R. Pinkas-Kramarski, M.L.M. Van De Poll, M.J.H. Van Vugt, L.N. Klapper, E. Tzahar, H. Waterman, M. Sela, E.J.J. Van Zoelen, Y. Yarden, Differential endocytic routing of homo- and hetero-dimeric ErbB tyrosine kinases confers signaling superiority to receptor heterodimers, EMBO J. 17 (1998) 3385–3397. doi:10.1093/emboj/17.12.3385.

[17] Y. Yarden, M.X. Sliwkowski, Untangling the ErbB signalling network, Nat. Rev. Mol. Cell Biol. 2 (2001) 127–137. doi:10.1038/35052073.

[18] TYKERB (LAPATINIB DITOSYLATE), NDA: 022059, FDA Approv. Drug Prod. (n.d.). https://www.accessdata.fda.gov/scripts/cder/daf/.

[19] H. Shi, W. Zhang, Q. Zhi, M. Jiang, Lapatinib resistance in HER2+ cancers: latest findings and new concepts on molecular mechanisms, Tumor Biol. 37 (2016) 15411–15431. doi:10.1007/s13277-016-5467-2.

[20] GILOTRIF (AFATINIB DIMALEATE), NDA: 201292, FDA Approv. Drug Prod. (n.d.). https://www.accessdata.fda.gov/scripts/cder/daf/index.cfm?event=overview.proces s&ApplNo=201292.

[21] M.L. Sos, H.B. Rode, S. Heynck, M. Peifer, F. Fischer, S. Kluter, V.G. Pawar, C. Reuter, J.M. Heuckmann, J. Weiss, L. Ruddigkeit, M. Rabiller, M. Koker, J.R. Simard, M. Getlik, Y. Yuza, T.-H. Chen, H. Greulich, R.K. Thomas, D. Rauh, Chemogenomic Profiling Provides Insights into the Limited Activity of Irreversible EGFR Inhibitors in Tumor Cells Expressing the T790M EGFR Resistance Mutation, Cancer Res. 70 (2010) 868–874. doi:10.1158/0008-5472.CAN-09-3106.

[22] D. Ercan, K. Zejnullahu, K. Yonesaka, Y. Xiao, M. Capelletti, A. Rogers, E. Lifshits, A. Brown, C. Lee, J.G. Christensen, D.J. Kwiatkowski, J.A. Engelman, P.A. Jänne, Amplification of EGFR T790M causes resistance to an irreversible EGFR inhibitor, Oncogene. 29 (2010) 2346–2356. doi:10.1038/onc.2009.526.

[23] Y. Kim, J. Ko, Z. Cui, A. Abolhoda, J.S. Ahn, S.-H. Ou, M.-J. Ahn, K. Park, The EGFR T790M Mutation in Acquired Resistance to an Irreversible Second-Generation EGFR Inhibitor, Mol. Cancer Ther. 11 (2012) 784–791. doi:10.1158/1535-7163.MCT-11-0750.

[24] L. Coussens, T. Yang-Feng, Y. Liao, E. Chen, A. Gray, J. McGrath, P. Seeburg, T. Libermann, J. Schlessinger, U. Francke, A. Levinson, A. Ullrich, Tyrosine kinase receptor with extensive homology to EGF receptor shares chromosomal location

with neu oncogene, Science. 230 (1985) 1132–1139.
doi:10.1126/science.2999974.

[25] T. Yamamoto, S. Ikawa, T. Akiyama, K. Semba, N. Nomura, N. Miyajima, T. Saito, K. Toyoshima, Similarity of protein encoded by the human c-erb-B-2 gene to epidermal growth factor receptor., Nature. 319 (1986) 230–4. doi:10.1038/319230a0.

[26] K. Aertgeerts, R. Skene, J. Yano, B.-C. Sang, H. Zou, G. Snell, A. Jennings, K. Iwamoto, N. Habuka, A. Hirokawa, T. Ishikawa, T. Tanaka, H. Miki, Y. Ohta, S. Sogabe, Structural Analysis of the Mechanism of Inhibition and Allosteric Activation of the Kinase Domain of HER2 Protein, J. Biol. Chem. 286 (2011) 18756–18765. doi:10.1074/jbc.M110.206193.

[27] D.W. Rusnak, K. Affleck, S.G. Cockerill, C. Stubberfield, R. Harris, M. Page, K.J. Smith, S.B. Guntrip, M.C. Carter, R.J. Shaw, A. Jowett, J. Stables, P. Topley, E.R. Wood, P.S. Brignola, S.H. Kadwell, B.R. Reep, R.J. Mullin, K.J. Alligood, B.R. Keith, R.M. Crosby, D.M. Murray, W.B. Knight, T.M. Gilmer, K. Lackey, The characterization of novel, dual ErbB-2/EGFR, tyrosine kinase inhibitors: potential therapy for cancer., Cancer Res. 61 (2001) 7196–203.

[28] S. Cockerill, C. Stubberfield, J. Stables, M. Carter, S. Guntrip, K. Smith, S. McKeown, R. Shaw, P. Topley, L. Thomsen, K. Affleck, A. Jowett, D. Hayes, M. Willson, P. Woollard, D. Spalding, Indazolylamino quinazolines and pyridopyrimidines as inhibitors of the EGFr and c-erbB-2, Bioorg. Med. Chem. Lett. 11 (2001) 1401–1405. doi:10.1016/S0960-894X(01)00219-0.

[29] C.-H. Yun, K.E. Mengwasser, A. V Toms, M.S. Woo, H. Greulich, K.-K. Wong, M. Meyerson, M.J. Eck, The T790M mutation in EGFR kinase causes drug resistance by increasing the affinity for ATP, Proc. Natl. Acad. Sci. 105 (2008) 2070–2075. doi:10.1073/pnas.0709662105.

[30] J. Park, J.J. McDonald, R.C. Petter, K.N. Houk, Molecular Dynamics Analysis of Binding of Kinase Inhibitors to WT EGFR and the T790M Mutant, J. Chem. Theory Comput. 12 (2016) 2066–2078. doi:10.1021/acs.jctc.5b01221.

[31] P. Wipf, E.M. Skoda, A. Mann, Conformational Restriction and Steric Hindrance in Medicinal Chemistry, in: Pract. Med. Chem., 4th ed., Academic Press Burlington, MA, 2015: pp. 279–299.

[32] F. Fontana, A. Leganza, S. Osti, Impurity of lapatinib and salts thereof, EP2489661A1, 2012.

[33] S. Bugge, I.U. Moen, K.-O. Kragseth Sylte, E. Sundby, B.H. Hoff, Truncated structures used in search for new lead compounds and in a retrospective analysis of thienopyrimidine-based EGFR inhibitors, Eur. J. Med. Chem. 94 (2015) 175–194. doi:10.1016/j.ejmech.2015.03.004.

[34] T. Ishikawa, M. Seto, H. Banno, Y. Kawakita, M. Oorui, T. Taniguchi, Y. Ohta, T. Tamura, A. Nakayama, H. Miki, H. Kamiguchi, T. Tanaka, N. Habuka, S. Sogabe, J. Yano, K. Aertgeerts, K. Kamiyama, Design and Synthesis of Novel Human

Epidermal Growth Factor Receptor 2 (HER2)/Epidermal Growth Factor Receptor (EGFR) Dual Inhibitors Bearing a Pyrrolo[3,2- d]pyrimidine Scaffold, J. Med. Chem. 54 (2011) 8030–8050. doi:10.1021/jm2008634.

[35] F.D. Bellamy, K. Ou, Selective reduction of aromatic nitro compounds with stannous chloride in non acidic and non aqueous medium, Tetrahedron Lett. 25 (1984) 839–842. doi:10.1016/S0040-4039(01)80041-1.

[36] G.D. Vite, A. V. Gavai, B.E. Fink, H. Mastalerz, J.F. Kadow, C-6 modified indazolylpyrrolotriazines, EP1569937B1, 2011.

[37] M.G. Vetelino, J.W. Coe, A mild method for the conversion of activated aryl methyl groups to carboxaldehydes via the uncatalyzed periodate cleavage of enamines, Tetrahedron Lett. 35 (1994) 219–222. doi:10.1016/S0040-4039(00)76515-4.

[38] S. Al-Mousawi, M.S. Moustafa, M.H. Elnagdi, Studies with enamines: Functionally substituted enamines as aldehyde equivalents in Gewald reactions, Arkivoc. 10 (2008) 17–25. doi:10.3998/ark.5550190.0009.a03.

[39] Y. Kawakita, H. Banno, T. Ohashi, T. Tamura, T. Yusa, A. Nakayama, H. Miki, H. Iwata, H. Kamiguchi, T. Tanaka, N. Habuka, S. Sogabe, Y. Ohta, T. Ishikawa, Design and Synthesis of Pyrrolo[3,2- d]pyrimidine Human Epidermal Growth Factor Receptor 2 (HER2)/Epidermal Growth Factor Receptor (EGFR) Dual Inhibitors: Exploration of Novel Back-Pocket Binders, J. Med. Chem. 55 (2012) 3975–3991. doi:10.1021/jm300185p.

[40] P. Politzer, P. Lane, M.C. Concha, Y. Ma, J.S. Murray, An overview of halogen bonding, J. Mol. Model. 13 (2007) 305–311. doi:10.1007/s00894-006-0154-7.

[41] B.K. Saha, A. Nangia, Ethynyl Group as a Supramolecular Halogen and C≡C–H···C≡C Trimer Synthon in 2,4,6-Tris(4-ethynylphenoxy)-1,3,5-triazine, Cryst. Growth Des. 7 (2007) 393–401. doi:10.1021/cg060744+.

[42] C.B. Aakeröy, D. Welideniya, J. Desper, Ethynyl hydrogen bonds and iodoethynyl halogen bonds: a case of synthon mimicry, CrystEngComm. 19 (2017) 11–13. doi:10.1039/C6CE02201D.

[43] S. Oae, J. Doi, Chapter 1: Sulfur Bonding, in: Org. Sulfur Chem. Vol. 1, CRC Press, 1991: pp. 1–30.

[44] F. Yamasaki, D. Zhang, C. Bartholomeusz, T. Sudo, G.N. Hortobagyi, K. Kurisu, N.T. Ueno, Sensitivity of breast cancer cells to erlotinib depends on cyclin-dependent kinase 2 activity, Mol. Cancer Ther. 6 (2007) 2168–2177. doi:10.1158/1535-7163.MCT-06-0514.

[45] N. Sagawa, T. Shikata, Are all polar molecules hydrophilic? Hydration numbers of nitro compounds and nitriles in aqueous solution, Phys. Chem. Chem. Phys. 16 (2014) 13262–13270. doi:10.1039/c4cp01280a.

[46] S.L. Holbeck, J.M. Collins, J.H. Doroshow, Analysis of Food and Drug Administration-approved anticancer agents in the NCI60 panel of human tumor

cell lines., Mol. Cancer Ther. 9 (2010) 1451–60. doi:10.1158/1535-7163.MCT-10-0106.

[47] L. Cai, W. Liu, J.-F. Ning, W.-Q. Meng, J. Hu, Y.-B. Zhao, C. Liu, Navigating into the binding pockets of the HER family protein kinases: discovery of novel EGFR inhibitor as antitumor agent, Drug Des. Devel. Ther. 9 (2015) 3837—3851. doi:10.2147/DDDT.S85357.

[48] T.T. Talele, The "Cyclopropyl Fragment" is a Versatile Player that Frequently Appears in Preclinical/Clinical Drug Molecules, J. Med. Chem. 59 (2016) 8712–8756. doi:10.1021/acs.jmedchem.6b00472.

[49] A.K. Abdel-Aziz, S.S.E. Azab, S.S. Youssef, A.M. El-Sayed, E. El-Demerdash, S. Shouman, Modulation of Imatinib Cytotoxicity by Selenite in HCT116 Colorectal Cancer Cells, Basic Clin. Pharmacol. Toxicol. 116 (2015) 37–46. doi:10.1111/bcpt.12281.

[50] A.K. Abdel-Aziz, S. Shouman, E. El-Demerdash, M. Elgendy, A.B. Abdel-Naim, Chloroquine synergizes sunitinib cytotoxicity via modulating autophagic, apoptotic and angiogenic machineries, Chem. Biol. Interact. 217 (2014) 28–40. doi:10.1016/j.cbi.2014.04.007.

Highlights

- A series of thieno[2,3-*d*]pyrimidine-based dual EGFR/HER2 inhibitors was developed.

- Screening for the optimum aniline headgroup for dual inhibition identified **21**.

- Optimizing the solubilizing group of **21** identified the promising dual inhibitor **27b**.

- **27b** showed dual EGFR/HER2 inhibition with IC_{50} of 91.7 nM and 1.2 μM, respectively.

- **27b** impeded NCI-H1975 (with T790M mutation) proliferation with IC_{50} of 4.2 μM.